UCIrvine
University of California, Irvine

Multidimensional Spectroscopy with Classical Fields vs Entangled Photons: Selecting Liouville Space Pathways

Shaul Mukamel ad Oleksiy Roslyak
Department of Chemistry, UCI, California

Kavli Institute for Theoretical Physics
Santa Barbara, CA
May 18, 2008

2D NMR Spectroscopy

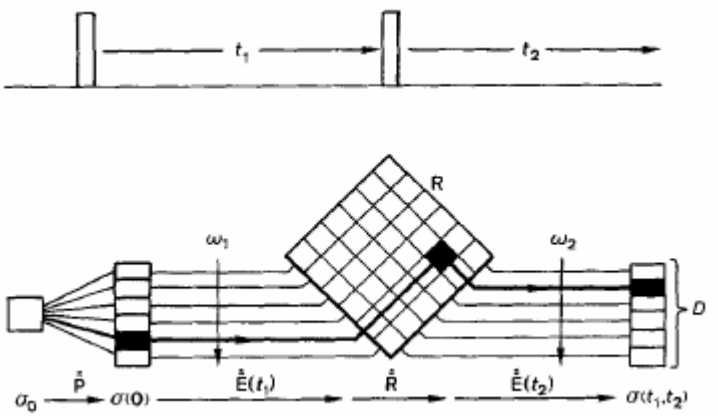

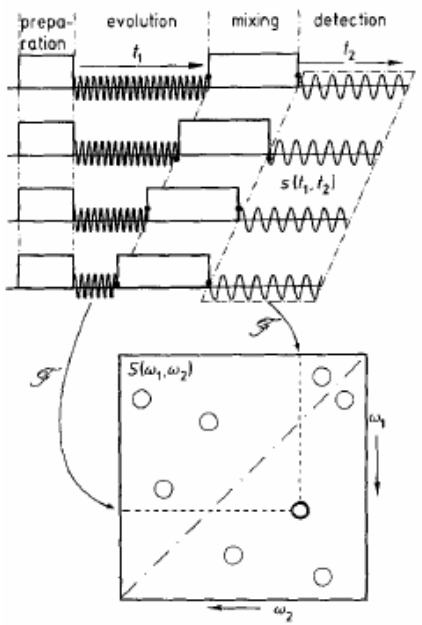

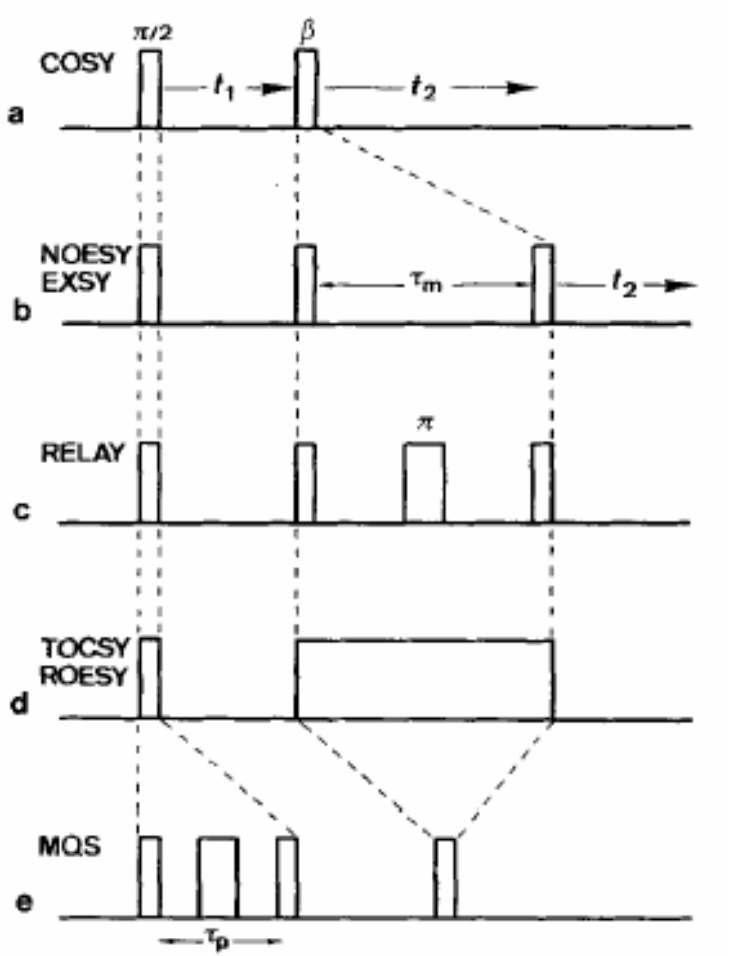

ANGEWANDTE
CHEMIE
International Edition in English

Volume 31 · Number 7
July 1992
Pages 805–930

Nuclear Magnetic Resonance Fourier Transform Spectroscopy (Nobel Lecture)**

By Richard R. Ernst*

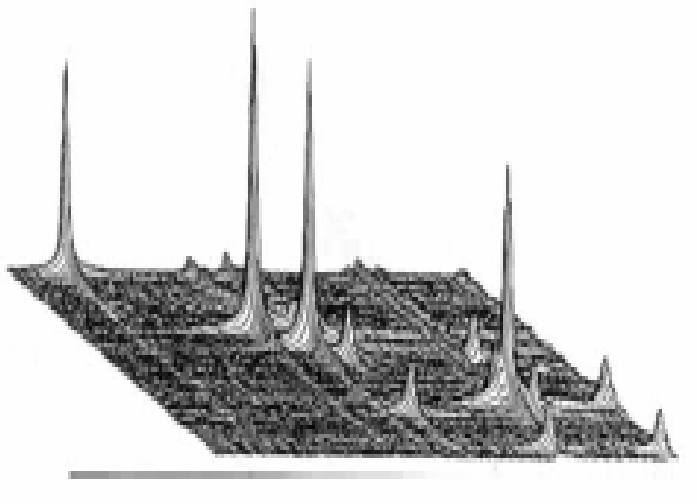

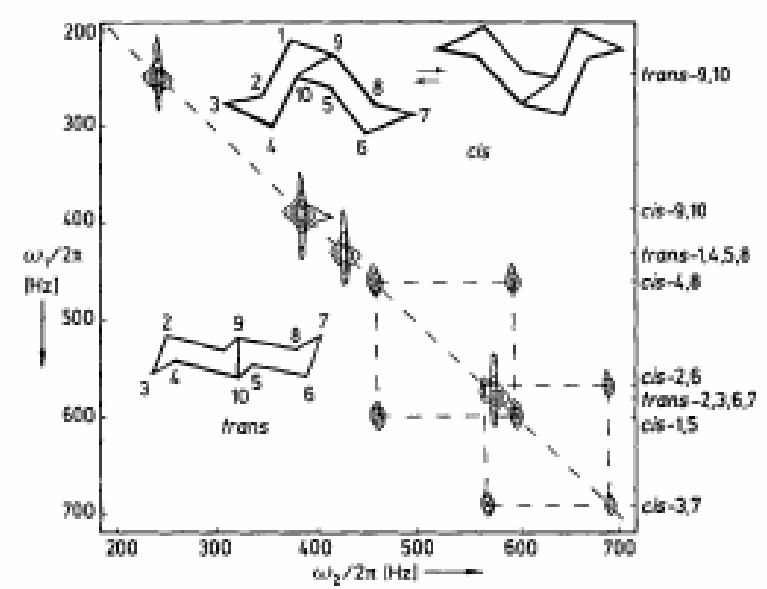

Heterodyne-Detected Four Wave Mixing

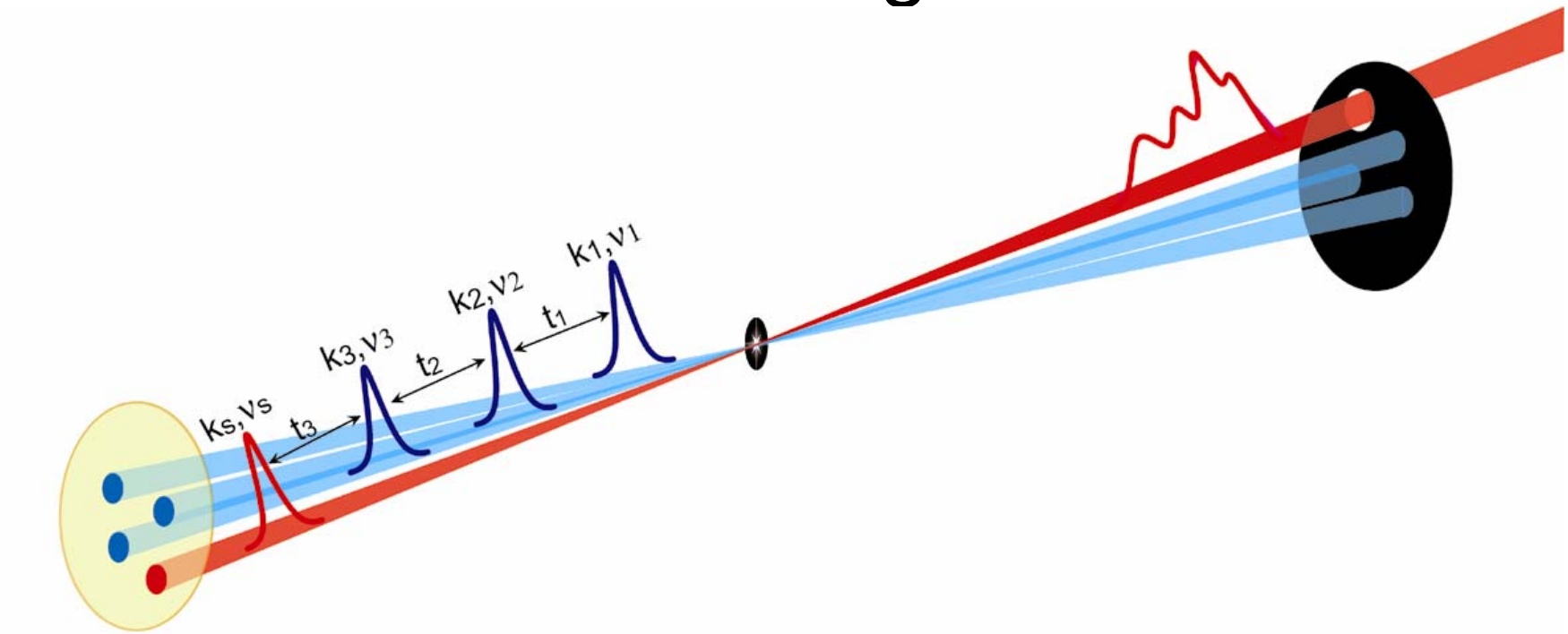

$$\boldsymbol{E}(\boldsymbol{r},\tau)=\sum_{j=1}^{4}\sum_{\nu}E_{j\nu}(\tau-\bar{\tau}_j)\exp[ik_j r-i\bar{\omega}_j(\tau-\bar{\tau}_j)-i\varphi_{j\nu}(\tau-\bar{\tau}_j)]+c.c.,$$

$$\boldsymbol{k_s}=\pm\boldsymbol{k_1}\pm\boldsymbol{k_2}\pm\boldsymbol{k_3}$$

Coherent (non) linear response to classical fields

(*n* + 1) wave mixing: *n* incoming fields generate 1 signal field (k_s)

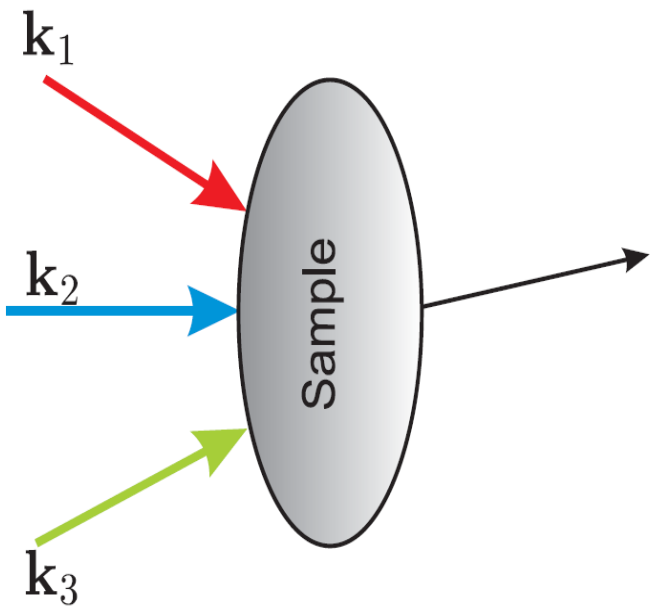

***n* incoming fields induce an *n*th order polarization $P^{(n)}$ in the material system**

Semi-classical theory:
material ↔ quantum
field ↔ classical

four-wave mixing (n=3)

The Nonlinear Response Functions

$$P(\mathbf{r},t) = P^{(1)}(\mathbf{r},t) + P^{(2)}(\mathbf{r},t) + P^{(3)}(\mathbf{r},t) + ...$$

Nonlinear polarization $P^{(n)}(\mathbf{r},t) \equiv \langle\langle V|\rho^{(n)}(t)\rangle\rangle \equiv Tr[V\rho^{(n)}(t)]$

$$P^{(n)}(\mathbf{r},t) = \int_0^\infty dt_n \int_0^\infty dt_{n-1} ... \int_0^\infty dt_1 S^{(n)}(t_n, t_{n-1}, ..., t_1)$$
$$\times E(\mathbf{r}, t-t_n) E(\mathbf{r}, t-t_n-t_{n-1}) ... E(\mathbf{r}, t-t_n-t_{n-1} ... -t_1),$$

$$S^{(3)}(t_3, t_2, t_1) = \left(\frac{i}{\hbar}\right)^3 \langle\langle V|\mathscr{G}(t_3)\mathscr{V}\mathscr{G}(t_2)\mathscr{V}\mathscr{G}(t_1)\mathscr{V}|\rho(-\infty)\rangle\rangle$$

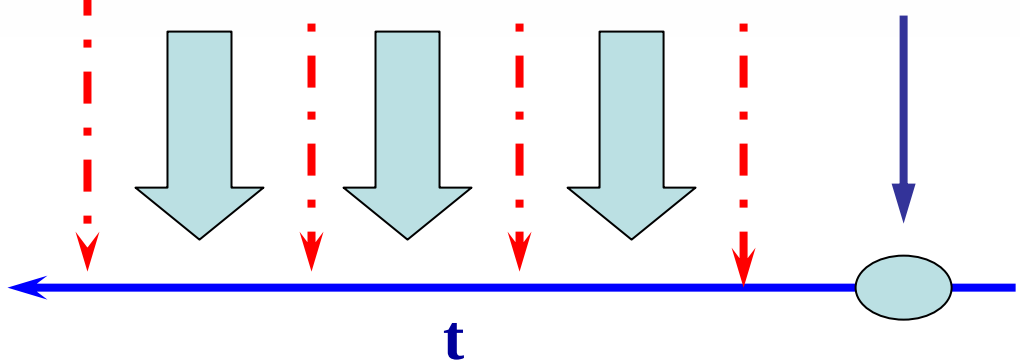

Two-dimensional correlation plots

- Double Fourier transform:

$$S_I(\Omega_1, t_2, \Omega_3) = \int_0^\infty dt_3 \int_0^\infty dt_1 e^{i\Omega_1 t_1 + i\Omega_3 t_3} S(t_1, t_2, t_3)$$

$$S_{III}(t_1, \Omega_2, \Omega_3) = \int_0^\infty dt_3 \int_0^\infty dt_2 e^{i\Omega_2 t_2 + i\Omega_3 t_3} S(t_1, t_2, t_3)$$

- Particularly useful for displaying structural information, in analogy with 2D NMR
- Ultrafast (50 fs) time resolution
- Probe intra- and intermolecular interactions
- Spreading transitions in multiple dimensions
- Lineshapes give environment fluctuations

Semi-classical prescription for calculating the signal

Two steps:

1. **microscopic step:**
   calculate the polarization,
   $P^{(n)}$, induced by the
   classical incoming fields

$$P^{(n)}(\mathbf{r},t) = \int \mathrm{d}t_n \int \ldots \int \mathrm{d}t_1$$
$$E(\mathbf{r}, t-t_n)\ldots E(\mathbf{r}, t-t_n-\cdots-t_1) S^{(n)}(t_n,\ldots,t_1)$$

$S^{(n)}$… nth order response function

2. Macroscopic step: solve Maxwell's equations with $P^{(n)}$ as a source

Multi wave-mixing & the phase-matching condition

.... Suppose we know $P^{(n)}$…

→ step 2: solve Maxwell eqn. for the signal field; $P^{(n)}$ serves as a source.

***N* incoming fields:** $$E(\mathbf{r},t)=\sum_{j=1}^{n}\left\{E_j(\mathbf{r},t)e^{i(\mathbf{k}_j\cdot\mathbf{r}-\omega_j t)}+\text{c.c.}\right\}$$

Solution depends on geometry (boundary conditions) and pulse configuration of the sample

$$\nabla^2 E(\mathbf{r},t)-\frac{n^2}{c^2}\frac{\partial^2}{\partial t^2}E(\mathbf{r},t)=\frac{4\pi}{c^2}\frac{\partial^2}{\partial t^2}P^{(n)}(\mathbf{r},t)$$

… yields a directed signal

Within the slowly varying amplitude approximation:

$$\Rightarrow \begin{cases} ik_{s,z}\dfrac{\partial E_s}{\partial z} = -\dfrac{2\pi}{c^2}\omega_c^2 P_c \mathrm{r}^{i\Delta k z} \\ \Delta k = (\mathbf{k}_c - \mathbf{k}_s)\cdot \hat{\mathbf{e}}_z \end{cases}$$

$\mathbf{k}_c = \pm\mathbf{k}_1 \pm \mathbf{k}_2 \pm \cdots \pm \mathbf{k}_n$, $\mathbf{k}_s$-signal

$$E_s(l,t) = \frac{2\pi i}{n(\omega_c)}\frac{\omega_c}{c} L P_c(t)\,\mathrm{sinc}\left(\frac{1}{2}\Delta k L\right) e^{i\frac{1}{2}\Delta k L}$$

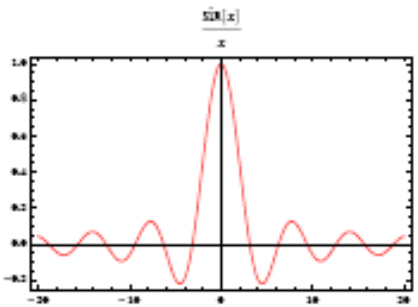

Phase matching condition:

$$\Delta k \stackrel{!}{=} 0$$

Detection modes

- **Homodyne detection: measure intensity**

$$I_s(t) = |E_s(\mathbf{r}, t)|^2$$

Heterodyne (holographic) detection: extract amplitude & phase of the field by interference of E_s with external field, E_{LO} ("local oscillator"), Propagating along k_s

$$S_{\mathrm{HET}} = |E_s + E_{\mathrm{LO}}|^2 - |E_{\mathrm{LO}}|^2 = |E_s|^2 + 2\mathrm{Re}(E_{\mathrm{LO}}^* E_s)$$

Since $|E_s|^2 \ll |E_{\mathrm{LO}}|^2$:

$$\boxed{S_{\mathrm{HET}} \sim \mathrm{Im}(E_{\mathrm{LO}}^* P_s(t))}$$

How to calculate the polarization?

(A) Wave function (Hilbert space) approach:

$$\boxed{|\dot{\psi}\rangle = -\frac{i}{\hbar}\hat{H}|\psi\rangle}$$

$$P^{(n)}(\mathbf{r},t) = \sum_{k=0}^{n}\left\langle \psi^{(n-k)}(t)|\hat{V}|\psi^{(k)}(t)\right\rangle = \sum_{k=0}^{n}(-1)^{n-k}\left(\frac{i}{\hbar}\right)^{n}$$

$$\int_{-\infty}^{t} d\tau_{k+1}\int_{-\infty}^{\tau_{k+1}} d\tau_{k+2}\int\ldots\int_{-\infty}^{\tau_{n-1}} d\tau_n \int_{-\infty}^{t} d\tau_k \int_{-\infty}^{t} d\tau_{k-1}\int\ldots\int_{-\infty}^{\tau_2} d\tau_1$$

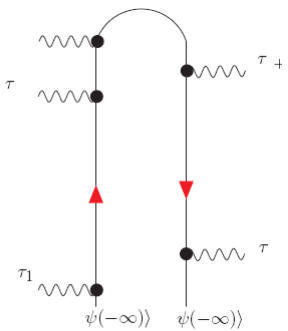

$$\langle\psi(-\infty)\ \hat{}\ (\tau_{k+1})\ \hat{}\ (\tau_{k+2})\qquad \hat{}\ (\tau_n)\ \hat{}\ (\ )\ \hat{}\ (\tau_k)\ \hat{}\ (\tau_{k-1})\qquad \hat{}\ (\tau_1)\ \psi(-\infty)\rangle$$

backward forward

Diagrammatic representation:
Schwinger-Keldysh loop

Forward & backward In time

(B) Density operator (Liouville space approach:

$$\dot{\hat{\rho}} = -\frac{i}{\hbar}\mathcal{L}\hat{\rho}$$

$$P^{(n)}(\mathbf{r},t) = \langle\langle \hat{V}|\hat{\rho}^{(n)}\rangle\rangle = \mathrm{Tr}\{\hat{V}\hat{\rho}^{(n)}\} = \int \mathrm{d}t_n \int \ldots \int \mathrm{d}t_1 \, E(\mathbf{r}, t-t_n)\ldots E(\mathbf{r}, t-t_n-\cdots-t_1)S^{(n)}(t_n,\ldots,t_1)$$

$$S^{(n)} = \langle\langle \hat{V}|\mathcal{G}(t_n)\mathcal{V}\mathcal{G}(t_{n-1})\mathcal{V}\ldots\mathcal{V}\mathcal{G}(t_2)\mathcal{V}\mathcal{G}(t_1)\mathcal{V}|\hat{\rho}(-\infty)\rangle\rangle$$

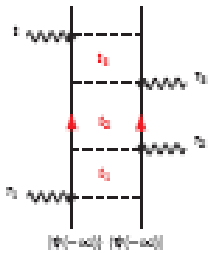

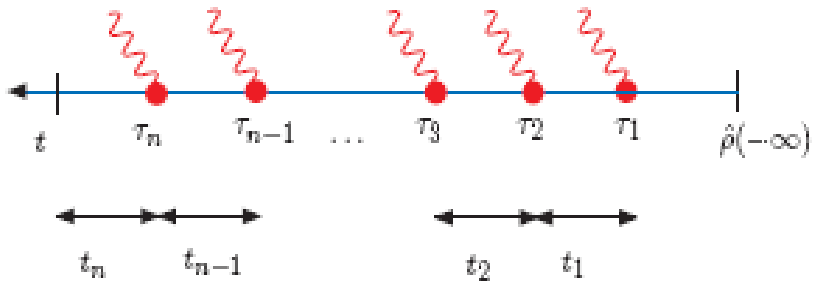

$$\mathcal{G}(t) = \theta(t)\exp\left(-\frac{i}{\hbar}\mathcal{L}t\right), \mathcal{V} = [\hat{V},.], \mathcal{L} = [\hat{H},.]$$

both bra and ket propagate forward in time

Diagrammatic representation: double sided Feynman diagram

Liouville-space pathways for third order response of excitons

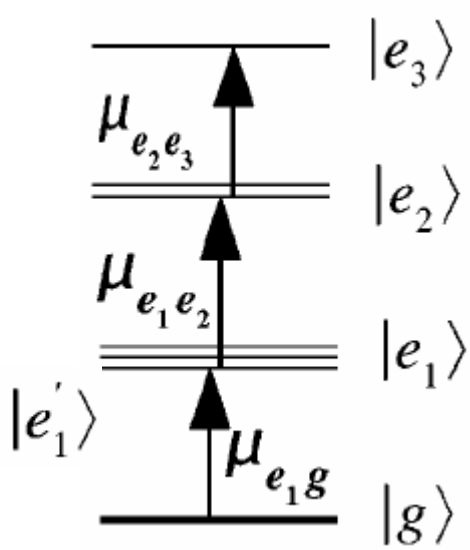

$$\mathbf{k}_I = -\mathbf{k}_1 + \mathbf{k}_2 + \mathbf{k}_3$$
$$\mathbf{k}_{II} = +\mathbf{k}_1 - \mathbf{k}_2 + \mathbf{k}_3$$
$$\mathbf{k}_{III} = +\mathbf{k}_1 + \mathbf{k}_2 - \mathbf{k}_3$$
$$\mathbf{k}_{IV} = +\mathbf{k}_1 + \mathbf{k}_2 + \mathbf{k}_3$$

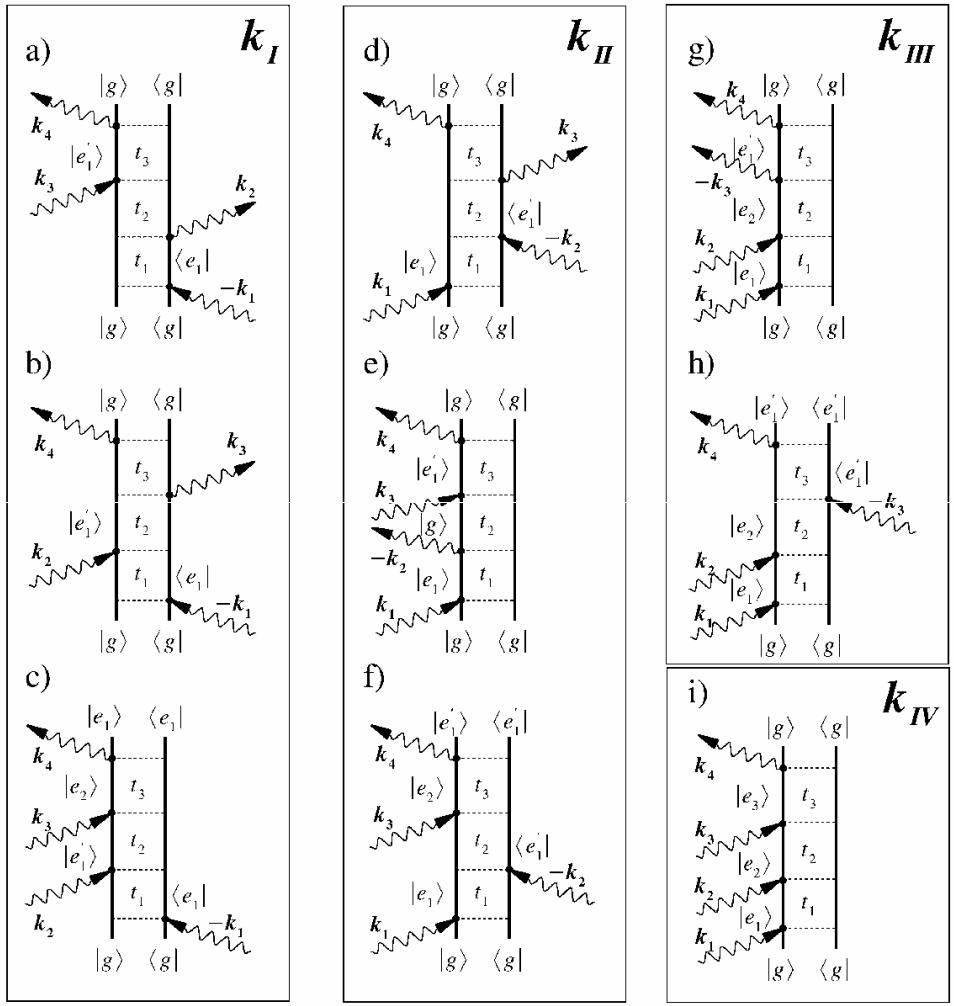

Merits of Liouville space picture

- We work in real physical time; purely forward propagation.
- The double sided Feynman diagrams connect directly to time-domain experiments.
- One explicitly visualizes the real time-intervals, t_j.

the $\boldsymbol{k_1 = -k_1 + k_2 + k_3}$ *- signal*

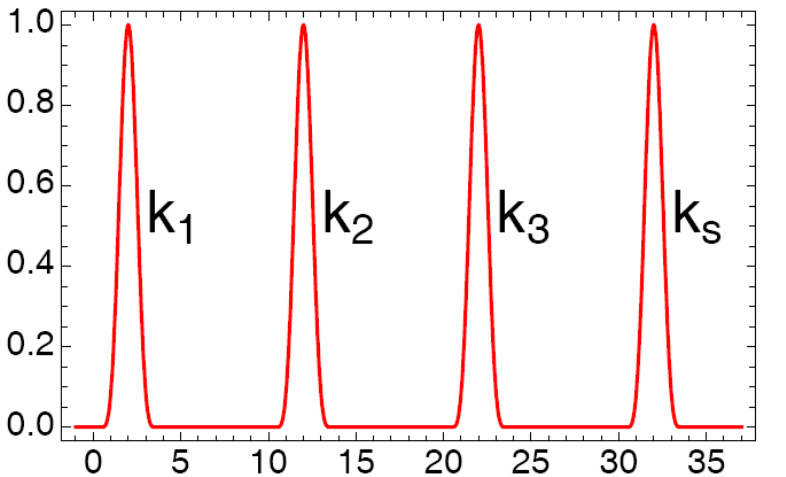

- **four wave mixing**
- **phase-matching direction:**
  $\mathbf{k_1 = -k_1 + k_2 + k_3}$
- **ideal time domain experiment with temporally well separated pulses**

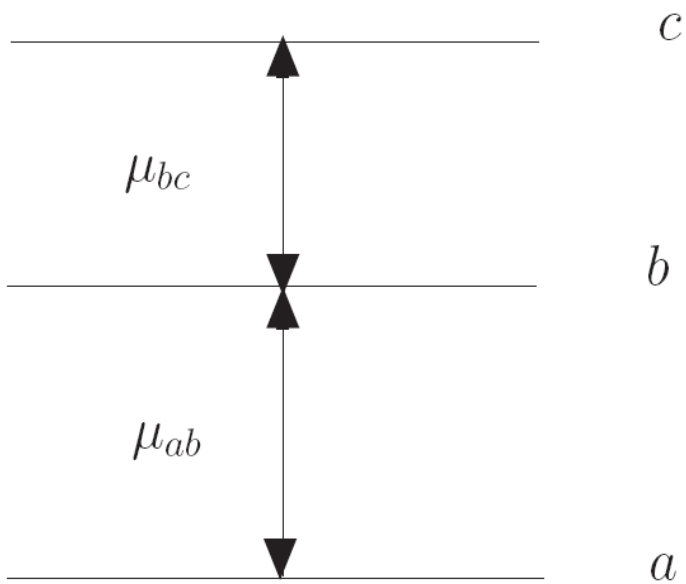

Three level model system

Double sided Feynman diagrams for the $\mathbf{k}_1$-signal

Rotating Wave approximation: photon absorption (“arrow pointing inwards”) excites the material, emission (“arrow pointing outwards”) de-excites the material.

3 Liouville space pathways: $I_{\nu\nu'}(t) = \theta(t) e^{-i\omega_{\nu\nu'}t - \gamma_{\nu\nu'}}$

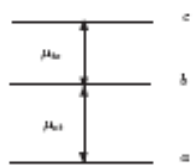

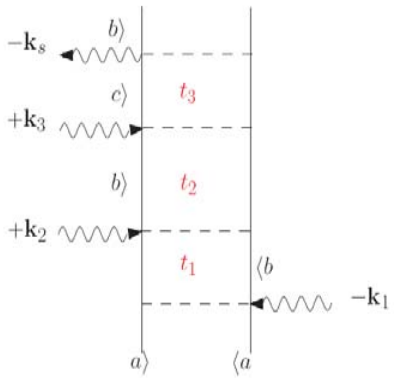

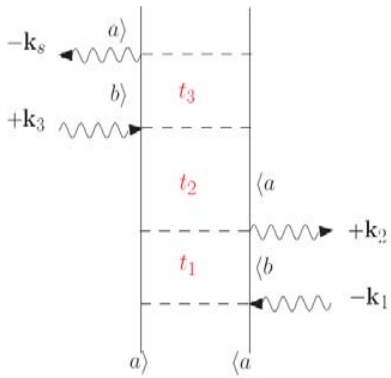

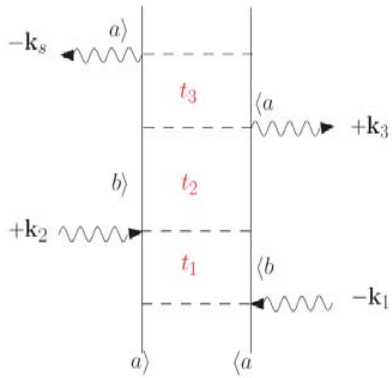

$$R_i = -\mu_{bc}\mu_{cb}\mu_{ba}\mu_{ab} \; I_{ab}(t_1) I_{bb}(t_2) I_{cb}(t_3)$$

$$R_{ii} = \mu_{ab}\mu_{ba}\mu_{ab}\mu_{ba} \; I_{ab}(t_1) I_{aa}(t_2) I_{ba}(t_3)$$

$$R_{iii} = \mu_{ab}\mu_{ba}\mu_{ab}\mu_{ba} \; I_{ab}(t_1) I_{bb}(t_2) I_{ba}(t_3)$$

$$P_{\mathbf{k}_I} = E_1^* E_2 E_3 S_{\mathbf{k}_I} \;,\; S_{\mathbf{k}_I} = \left(\frac{i}{\hbar}\right)^3 (R_i + R_{ii} + R_{iii})$$

Quantum description of Field

Hamiltonian of the joint matter-field system (the bare field, $\hat{H}_F = \sum_j \hbar\omega_j \hat{a}_j^\dagger \hat{a}_j$ is eliminated by going to the interaction picture)

$$\hat{H}(t) = \underbrace{\hat{H}_M}_{\text{… bare material}} + \underbrace{\hat{H}_{\text{int}}(t)}_{\text{… matter-field coupling}}$$

Replace classical field by field operator:

$$\hat{E}(\mathbf{r}, t) = \hat{\mathcal{E}}(\mathbf{r}, t) + \hat{\mathcal{E}}^\dagger(\mathbf{r}, t) \ ,$$

$$\hat{\mathcal{E}}(\mathbf{r}, t) = \sum_j \left(\frac{2\pi\hbar\omega_j}{\Omega}\right)^{1/2} \hat{a}_j e^{i\mathbf{k}_j\cdot\mathbf{r} - i\omega_j t}$$

photon field annihilation **operator, represents destruction of a photon at position r and time *t*.**

Photons are bosons: $[\hat{a}_j, \hat{a}_{j'}^\dagger] = \delta_{jj'}$

Matter-field coupling

Within the dipole – and Rotating Wave approximation

$$\hat{H}_{int}(t) = \underbrace{\hat{\mathcal{E}}(\mathbf{r},t)\hat{V}^{\dagger}}_{\text{... matter excited, photon destroyed}} + \underbrace{\hat{\mathcal{E}}^{\dagger}(\mathbf{r},t)\hat{V}}_{\text{... matter de-excited, photon created}}$$

Decompose dipole operator $\hat{\mu}$ according to

$$\hat{\mu} = \hat{V}^{\dagger} + \hat{V}$$

$$\hat{V}^{\dagger} = \sum_{k}\sum_{j>k} \mu_{jk} |j\rangle\langle k|$$

… raising operator: creates excitation in the material

$\hat{V}$ **… annihilates an excitation**

The optical signal

The detector registers the number of photons per unit time in mode α . The signal is given by the time averaged photon flux:

$$S_\alpha = \lim_{T\to\infty} \frac{1}{2T} \int_{-T}^{T} \frac{d}{dt} \left\langle a_\alpha^\dagger a_\alpha \right\rangle dt$$

The Heisenberg equation of motion for the photon number:

$$\frac{d}{dt} a_\alpha^\dagger a_\alpha = \frac{i}{\hbar} \left[H_{int}, a_\alpha^\dagger a_\alpha \right]$$

and the interaction Hamiltonian (1) give the following signal:

$$S_\alpha = \frac{1}{\pi\hbar} \Im \int_{-\infty}^{\infty} \left\langle E'_\alpha(t) V'_\alpha(t) \right\rangle dt \qquad E'_\alpha \propto a_\alpha^\dagger + a_\alpha$$

The expectation value $\left\langle \quad \right\rangle_\alpha$ is over the initial state of the entire system (light+matter)

Heterodyne detection revisited: a quantum field perspective

Semi-classical picture: Local oscillator (LO) does not interact with the material but only interferes with the generated signal field. We measure the change in intensity of the local oscillator.

Is this assumption of a spatially separated LO necessary?

In a quantum description we consider the whole process as a single (n + 1)-photon event with n + 1fields. The LO is singled out only by the detection process.

Calculate the change in intensity, S*T* directly from our microscopic definition of the signal,

$$S_T = \int_{-\infty}^{+\infty} S(\tau)\mathrm{d}\tau \quad \ldots \text{ time integrated signal}$$

$$S(t) = \frac{\mathrm{d}}{\mathrm{d}t}\left(\hat{a}_s^\dagger \hat{a}_s\right)_T$$

Heterodyne detection is a stimulated process by the local oscillator

Using Heisenberg's equation:

$$S(t) = \frac{2}{\hbar}\mathrm{Im}\left\{\left(\hat{\mathcal{E}}_s^{\dagger}(\mathbf{r},t)\hat{V}\right)_{\mathrm{T}}\right\}$$

→ this is the starting point for a perturbative expansion in all the modes (incoming & LO)

This looks like exactly like the semi-classical expression for the heterodyne detected signal, $S_{\mathrm{HET}} \sim \mathrm{Im}(E_{\mathrm{LO}}^{*} P_s(t))$ If we replace the field operatory, $\hat{\mathcal{E}}_s$ by a classical field.

Leading order contribution – each mode enters to first order.

Replacing $\hat{\mathcal{E}}_s$ by $\mathcal{E}_s^{*}$ Is exact!

The perturbative expansion

Perturbative expansion in the interaction Liouvillian superoperator $\left(H_{\text{int}}\right)_{-}$

$$S_{\alpha} = \sum_{m=1}^{\infty} S_{\alpha}^{(m)}$$

m wave mixing signals are given by products of material and corresponding optical field SNGF's of m-th order:

$$S_{\alpha}^{(m)} = \Im \frac{i^{m} \delta_{m+1,\alpha}}{\pi m! \hbar^{m+1}} \sum_{\nu_m} \cdots \sum_{\nu_1} \int_{-\infty}^{\infty} dt_{m+1} dt_m \ldots dt_1$$

$$\Theta(t_{m+1}) \mathrm{V}^{(m)}_{\nu_{m+1}\nu_m \ldots \nu_1}\left(t_{m+1}, t_m, \ldots, t_1\right) \mathrm{E}^{(m)}_{\nu_{m+1}\bar{\nu}_m \ldots \bar{\nu}_1}\left(t_{m+1}, t_m, \ldots, t_1\right)$$

In +,- representation: $\nu_j = \{+,-\}, \quad \bar{\nu}_j = \{-,+\}$

In L,R representation: $\nu_j = \{L,R\}, \quad \bar{\nu}_j = \{L,R\}$

The **optical** field SNGF's :

$$\mathrm{E}^{(m)}_{\nu_{m+1}\bar{\nu}_m \ldots \bar{\nu}_1}\left(t_{m+1}, t_m, \ldots, t_1\right) =$$

$$\langle \mathrm{T} E'_{\nu_{m+1}}(t_{m+1}) E'_{\bar{\nu}_m}(t_m) \ldots E'_{\bar{\nu}_1}(t_1) \rangle$$

The **material** SNGF's :

$$\mathrm{V}^{(m)}_{\nu_{m+1}\nu_m \ldots \nu_1}\left(t_{m+1}, t_m, \ldots, t_1\right) =$$

$$\langle \mathrm{T} V'_{\nu_{m+1}}(t_{m+1}) V'_{\nu_m}(t_m) \ldots V'_{\nu_1}(t_1) \rangle$$

Conclusions

Recover the classical result, but now LO does not have to be spatially separated anymore.

“One shot” microscopic calculation of the signal as an (n + 1)-photon event: no need to create polarization and use Maxwell equations.

UCIrvine
University of California, Irvine

Manipulating Quantum Pathways of Matter by Coherent Multidimensional Spectroscopy with Entangled Photons

The $k_s = -k_1+k_2+k_3$ - signal

Frequency domain; no control over time-ordering (different than k_I)

$$-\mathbf{k}_1 + \mathbf{k}_2 + \mathbf{k}_3 - \mathbf{k}_s = 0$$

Construction of the diagrams:

1. "2" and "3" are represented by arrows pointing to the right (absorption) and "1" and "s" by arrows pointing to the left (emission).
2. Consider all possible ways to distribute these arrows around the loop; Constraints:

- The interaction with the detected mode "s" is fixed to the top left branch.
- The material system must start & end in the same state (its ground state, |a>)

8 loop diagrams….

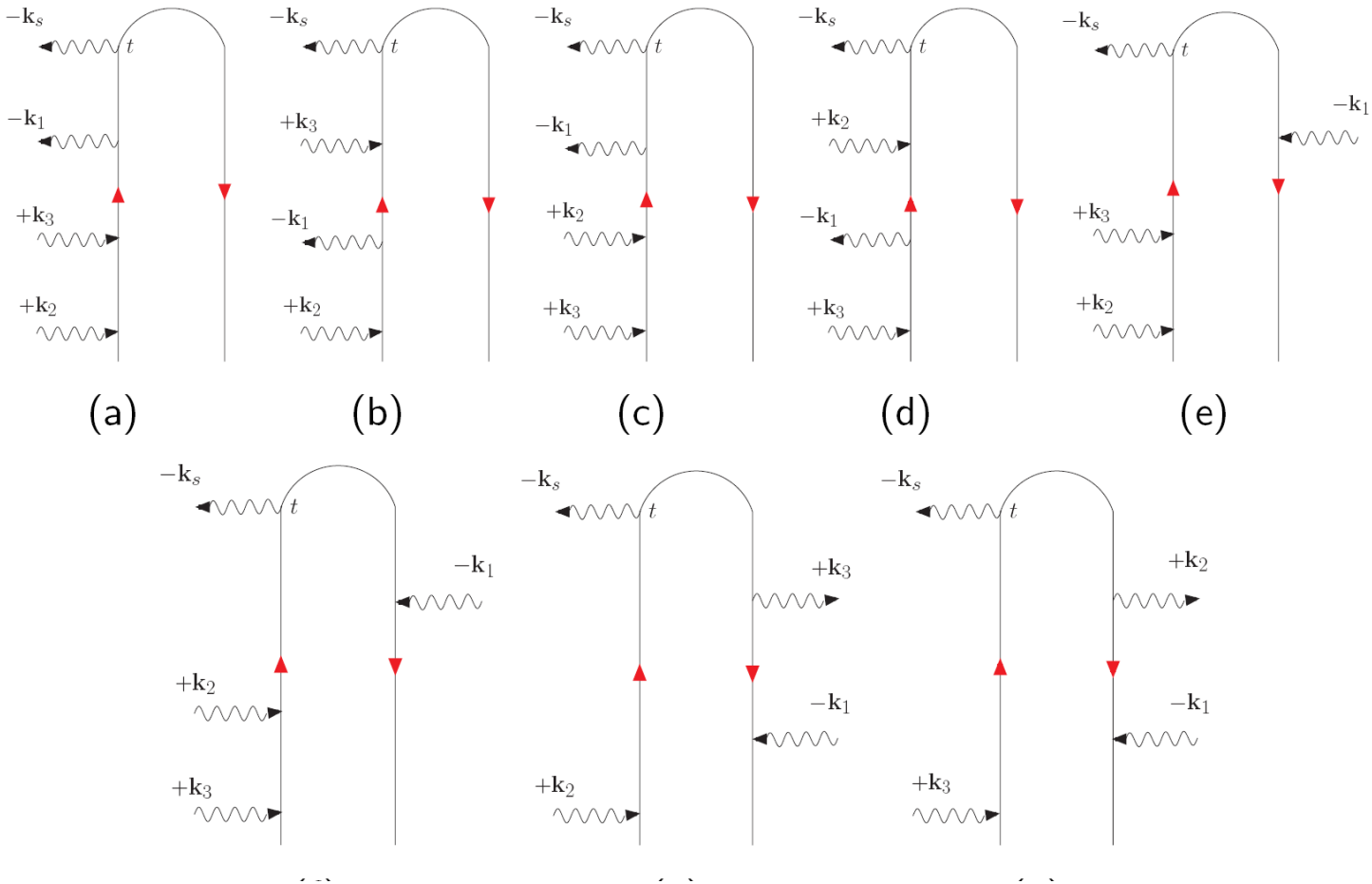

Twin entangled photons generated by PDC

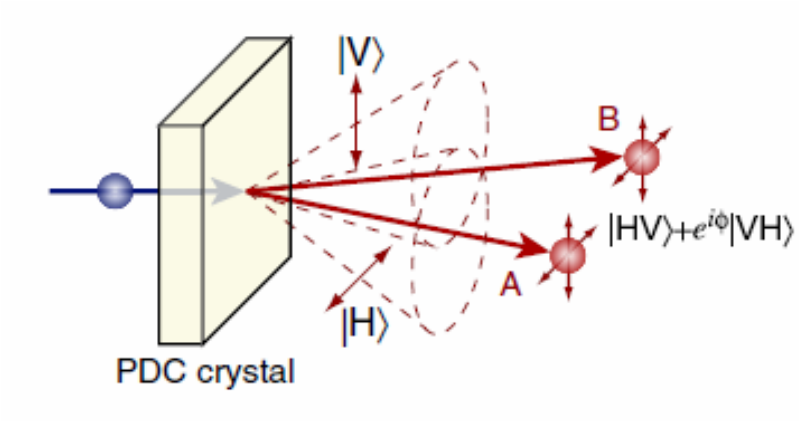

The idler (A = $\mathbf{k}_1$) and signal (B = $\mathbf{k}_2$) are populated from the vacuum state from the pump photon (P = $\mathbf{k}_0$) by means of the interactions mediated by the nonlinear $\chi^{(2)}$ crystal:

$$H_{\text{int}}: \quad \chi^{(2)}\left(a_1^{\dagger}a_2^{\dagger}a_0 + a_0^{\dagger}a_2 a_1\right)$$

The idler and signal are entangled:

$$G^{(4)}\left(r_6t_6,...,r_1t_1\right) = Tr\{a(r_1t_1)a(r_2t_2)a(r_3t_3)a(r_4t_4)a^{\dagger}(r_5t_5)a^{\dagger}(r_6t_6)a^{\dagger}(r_7t_7)a^{\dagger}(r_8t_8)\rho\} \neq 0$$

Twin photons. Types of entanglement.

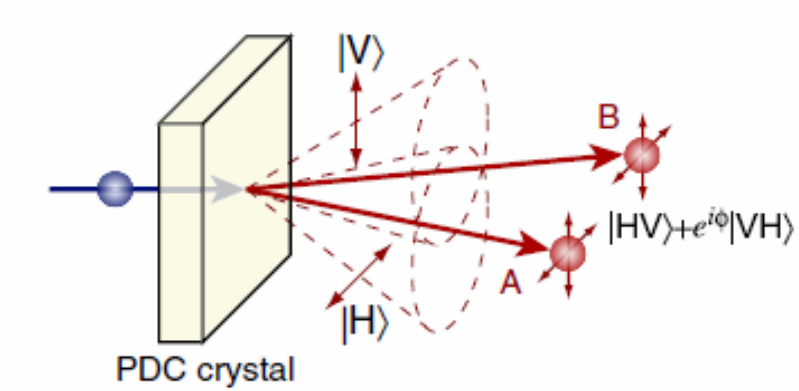

Polarization entanglement.

Photons having horizontal ($|H\rangle$, signal $\mathbf{k}_2$) and vertical ($|V\rangle$, idler $\mathbf{k}_1$) linear polarizations are emitted along the two conical surfaces. A pair of photons emitted to the crossing directions of the two cones is entangled.

Twin photons. Types of entanglement.

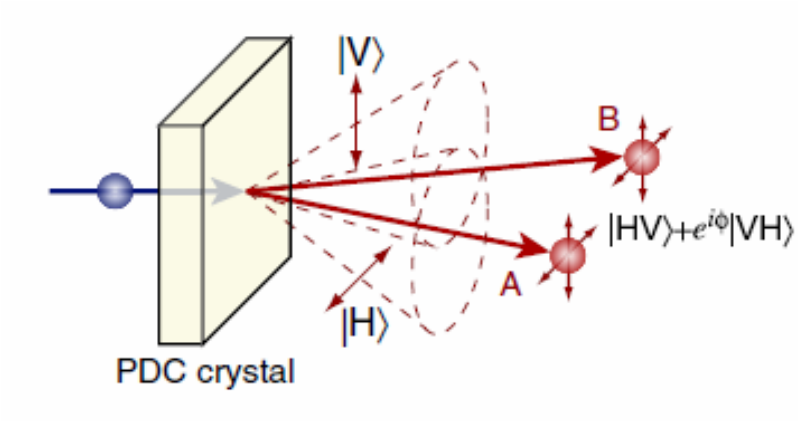

The twin photons are also entangled with respect to the continous variables:
position (space entanglement), frequency (energy entanglement),
wave vector (momentum entanglement).

$$|\psi\rangle = \int f\left(\omega_1(\mathbf{k}_1), x_1, \omega_2(\mathbf{k}_2), x_2\right) \left|\omega_1(\mathbf{k}_1), x_1\right\rangle \left|\omega_2(\mathbf{k}_2), x_2\right\rangle d\omega_1 d\omega_2 dx_1 dx_2$$

where f is a nonseparable function that depands on the phase matching condition:

$$\begin{cases} \omega_0 = \omega_1 + \omega_2 \\ \mathbf{k}_0 = \mathbf{k}_1 + \mathbf{k}_2 \end{cases}$$

Twin photons. Properties.

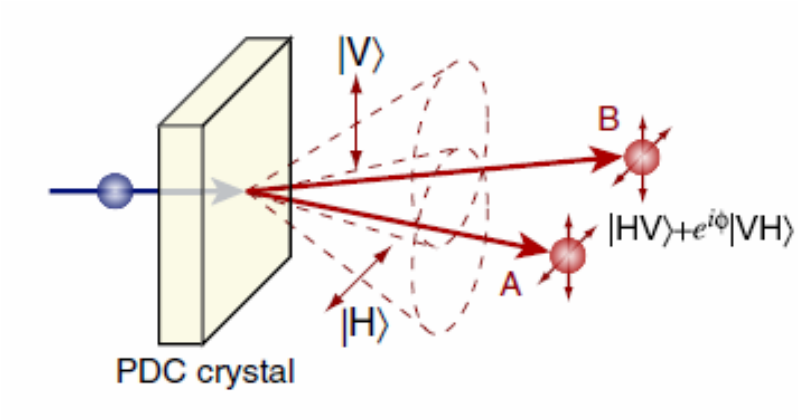

The twin photons are created withing an entanglement time T_{12} and within an entanglement area A_{12} of each other. This quantities represent the width of the fourth-order temporal- and spacial - coherence functions $G^{(4)}$, respectively.

Spectroscopy with Twin photons

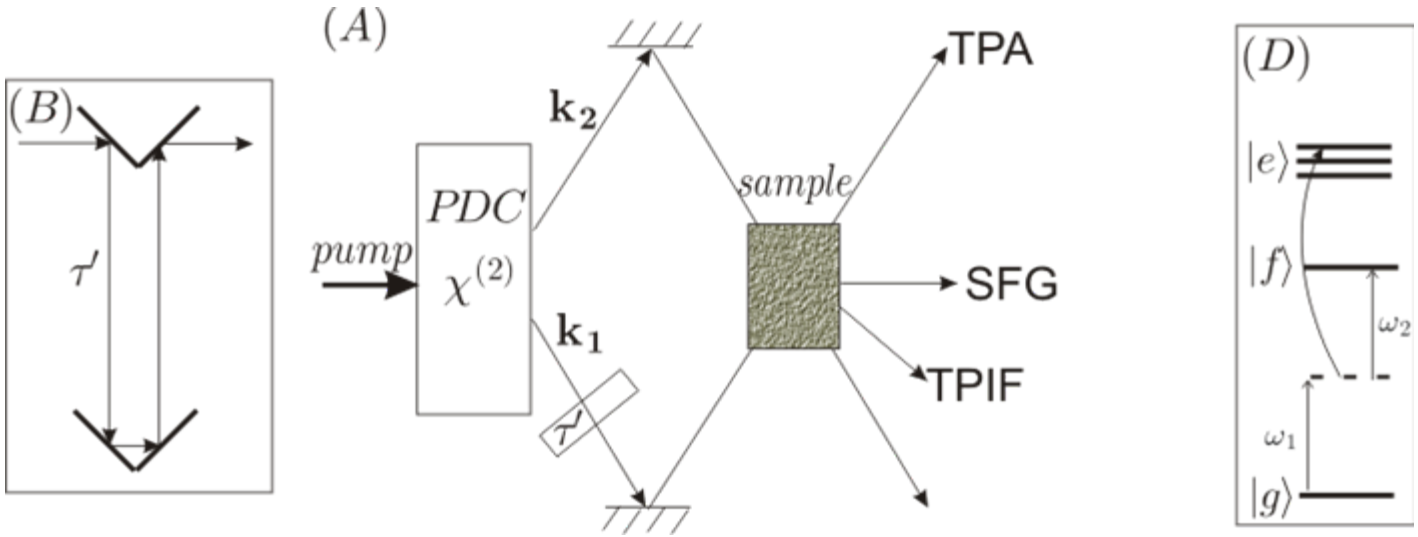

Several spectroscopic techniques had been reported by several groups:

Two photon absorption {Dayan 2004, Saleh 1998epv} (TPA),

Sum frequency generation {Silberberg 2007, Peer 2007} (SFG),

Two photon induced fluorescence {Goodgon_2007, Lee 2007, Teich_1998} (TPIF)

Signal linear dependence on pump intensity as a signature of entanglement.

$$S_{CL} \propto |E_1|^2 |E_2|^2, \qquad S_{EN} \propto |E_p|^2$$

Theoretical prediction for homodyne-detected SFG:

B. Saleh, B. Jostm, M. Teich: "*Entangled-Photons Virtual-State spectroscopy* "
PRL,80, 3483-3486, (1998).

A. Sergienko, M. Teich etc. "Quantum theory of entangled photon photoemission"
PRB, 69, 165317, (2004).

Experimental verification for homodyne-detected SFG and TPIF:

M. Teich, B. Saleh, "*Entangled-photons microscopy, spectroscopy and display*",
US Patent 5,796, 477

A.Pe'er, B. Dayan, Y.Silberberg, "*Temporal shaping of entangled photons*",
PRL, 94,073601 (2005), "*Nonlinear interactions with an ultrahigh flux of Broadband entangled photons*", PRL, 94, 043602 (2005).

D.Lee, T.Goodson "*Entangled Photon Absorption in an organic porphyrine dendrimer*", Journal of physical chemistry, 110, 25582-25585, (2006).

UCIrvine
University of California, Irvine

Improvements over conventional microscopy

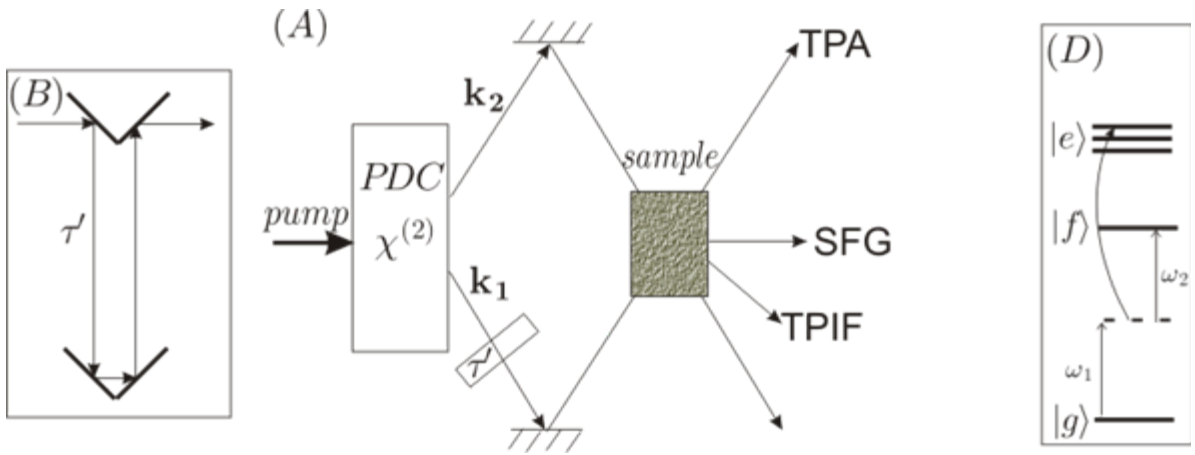

The absorption no longer depends on an accidentally simultaneous arrival of two photons. The twin photons act as a single unit and their absorption rate no longer quadratically depends on photon flux density, but appears to be linear {Javanainen 1990}.

$$\text{Absorption rate} : \frac{|E_p|^2}{T_{12} A_{12}}$$

Power levels required for TP excitation can be dramatically reduced

Spectral resolution can be improved since absorption only occur in a region where correlated photon pairs overlap in space.

Entangled photons PDC/MZI in non-linear spectroscopy

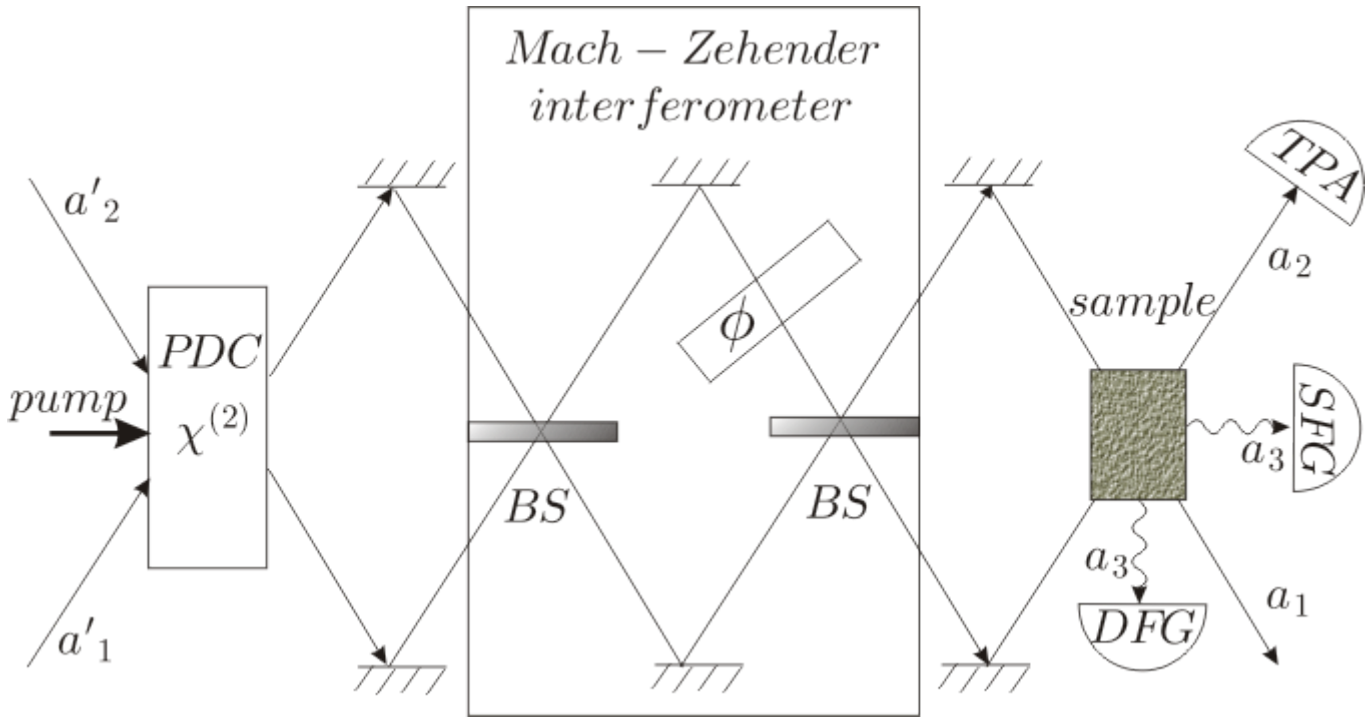

Experiments are conducted with the non-orthogonal modes a1, a2 with wavevectors **k**1,**k**2.

UCIrvine
University of California, Irvine

TPA

Pump-probe (PP) technique carried out with two optical modes Interacting with N three level molecules.

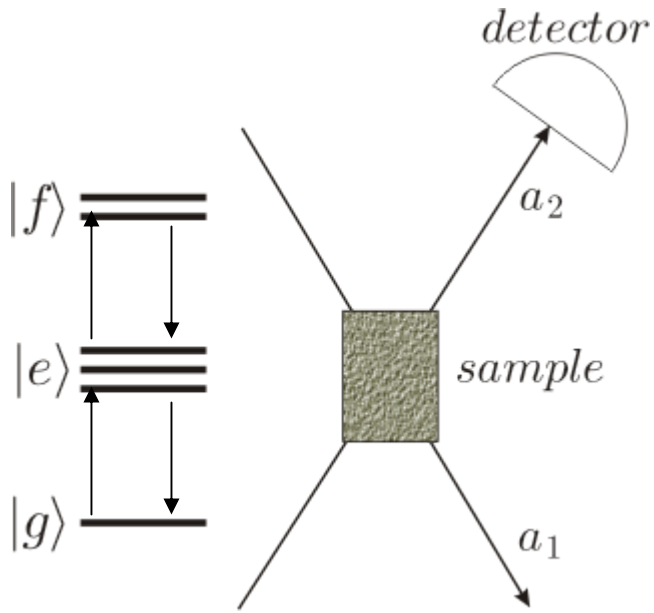

The signal is the time-averaged photon flux in one of the modes.

$$S(\omega_1, \omega_2) \propto \sum \text{material SNGF} \times \text{optical SNGF}$$

Pump-Probe with classical beams

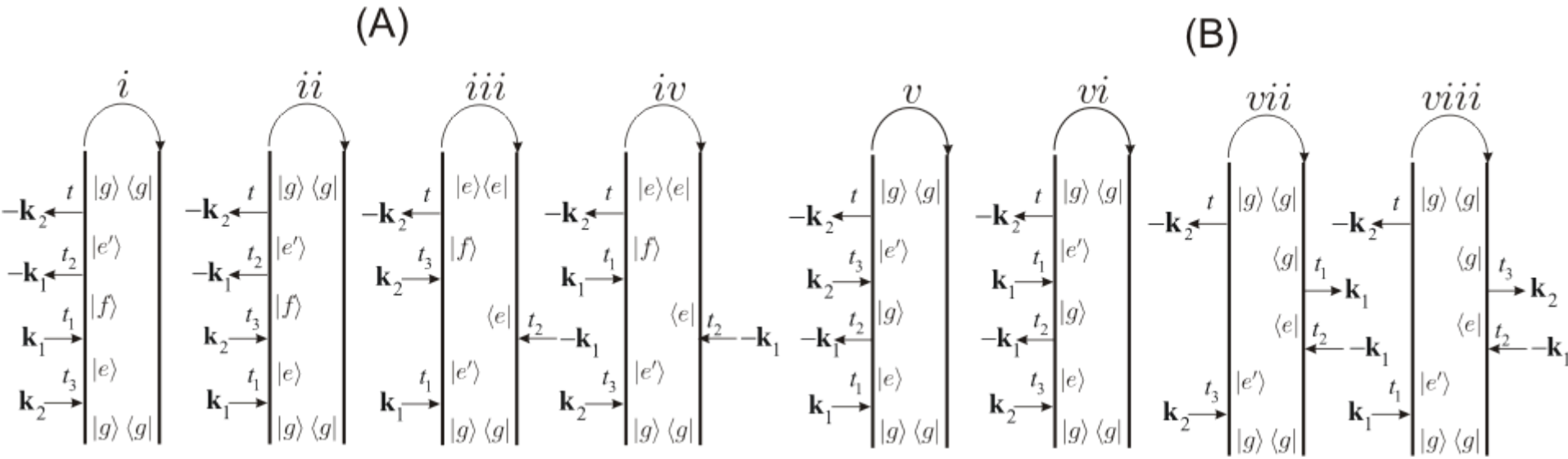

All optical SNGF's are the same: $\langle a_1 \rangle \langle a_2 \rangle \langle a_1^\dagger \rangle \langle a_2^\dagger \rangle \sim |\mathrm{E}_1|^2 |\mathrm{E}_2|^2$

The classical pump-probe signal is TPA + Ground state bleaching:

$$S^{(C)}(\omega_1, \omega_2) \sim |\mathrm{E}_1|^2 |\mathrm{E}_2|^2 \, \Im[\chi_A^{(3)}(\omega_1, \omega_2) + \chi_B^{(3)}(\omega_1, \omega_2)]$$

UCIrvine
University of California, Irvine

TPA with maximally entangled PDC/MZI beams

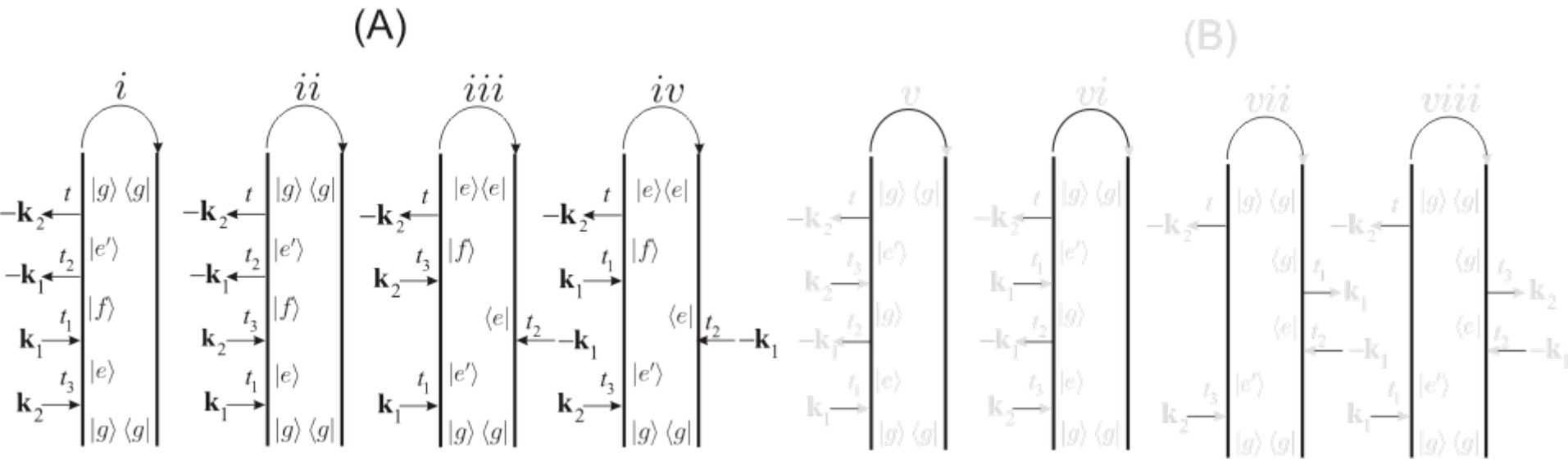

Optical SNGF's of group A:

$$\langle a^{\dagger}a^{\dagger}aa\rangle \sim |\mathrm{E}_p|^2 + |\mathrm{E}_p|^4$$

Optical SNGF's of group B:

$$\langle a^{\dagger}aa^{\dagger}a\rangle \sim |\mathrm{E}_p|^4$$

At low pump intensity limit the signal is solely given by group A :

$$S^{(E)}(\omega_1,\omega_2) \sim |\mathrm{E}_p|^2\, \Im\chi_A^{(3)}(\omega_1,\omega_2)$$

UCIrvine
University of California, Irvine

Group A TPA pathways contribution $\square |E_p|^2$

Cross peaks due to pathway *i* are given by double resonance condition:

$$\omega_2 \approx \omega_{eg},$$

$$\omega_1 + \omega_2 \approx \omega_{fg}$$

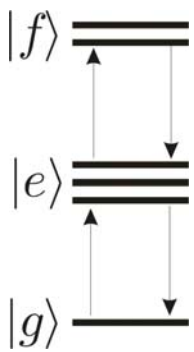

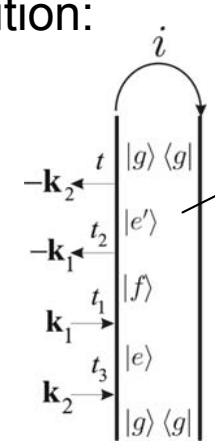

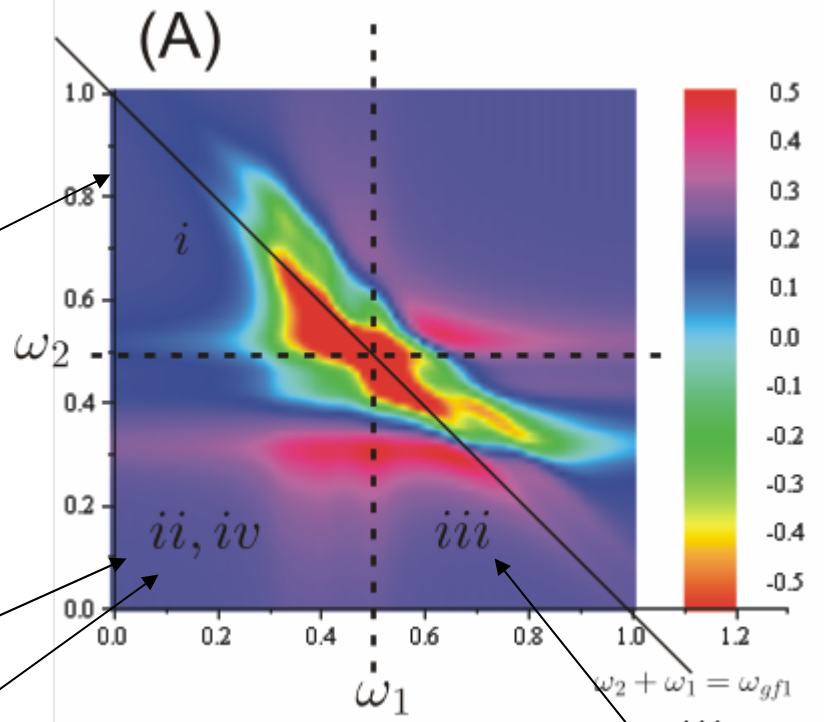

$$\omega_{eg} \approx \omega_{ef}$$

Cross peaks due to pathways *ii* and *iv* are given by triply resonant:

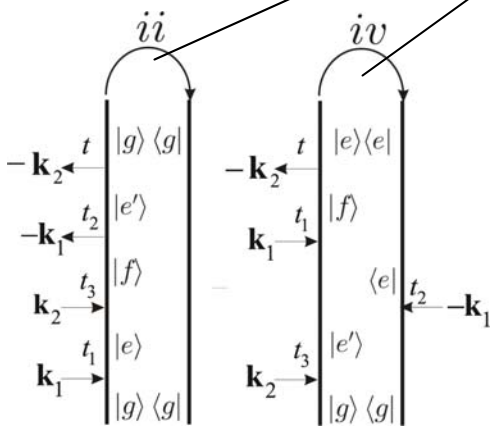

Cross-peaks due to pathway *iii* are doubly resonant:

$$\omega_1 \approx \omega_{eg},$$

$$\omega_1 + \omega_2 \approx \omega_{fg}$$

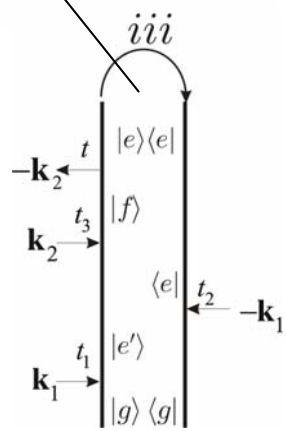

Group B Raman pathways contribution $\prod_p |E_p|^4$

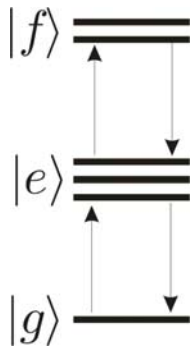

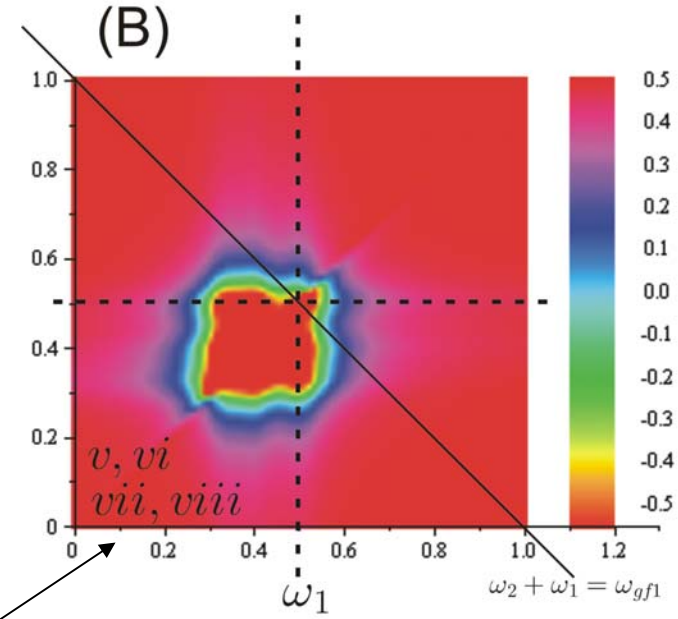

The pathways of group B induce cross-peaks at:

$$\omega_1 \approx \omega_{eg}, \quad \omega_2 \approx \omega_{e'g}$$

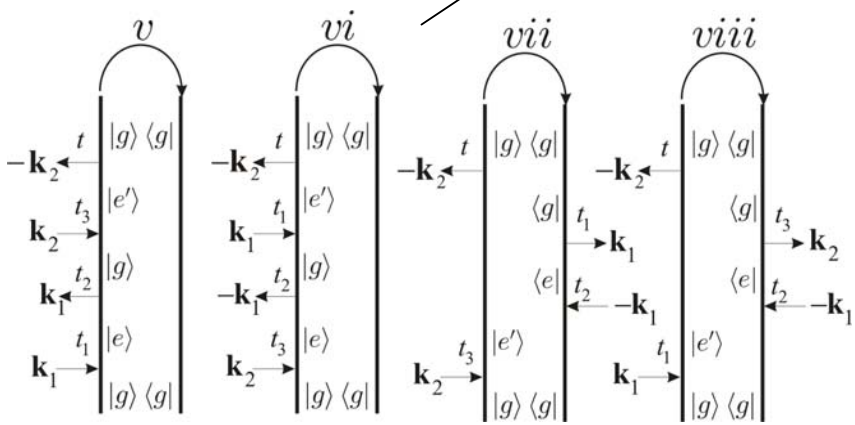

UCIrvine
University of California, Irvine

Total signal group A + B pathways

large dephasing rate and close transition frequencies:

$$\gamma / \omega_{eg} = 0.1$$

= Spectral overlap

$$\omega_{eg} \approx \omega_{fe}$$

All dipole moments are the same 0.1 (arb. units)

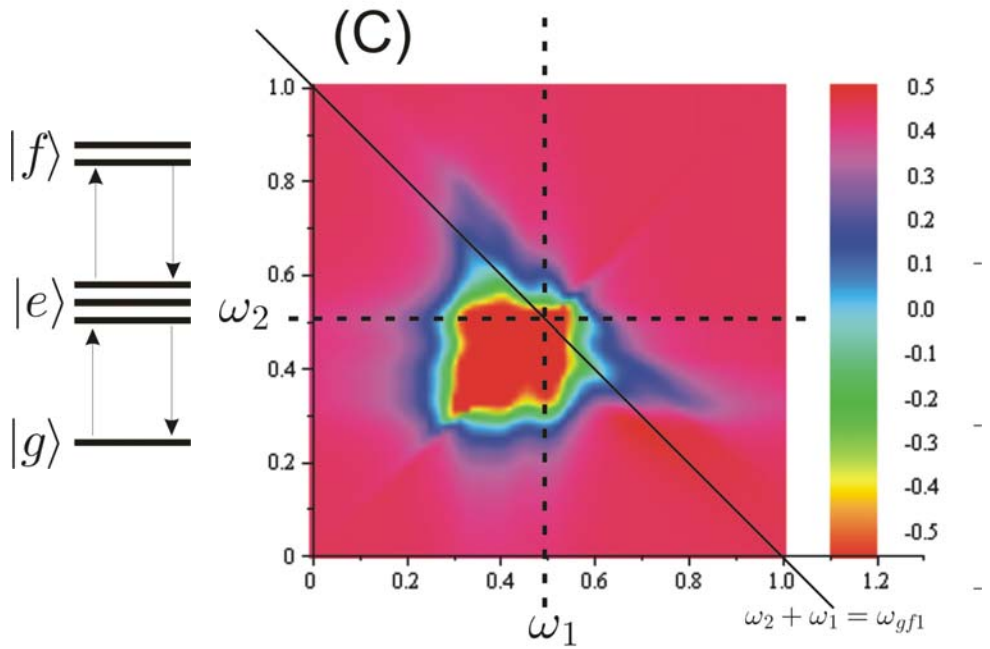

The pathways of group A (TPA) and B (single photon transition) may not be separated by using classical optical fields.

This is possible by the entangled (PDC/MZI) photon signal.

UCIrvine
University of California, Irvine

The diagonal section of the 2D spectra

A) Entangled photon (PDC/MZI) signal (Group A)
B) Group B contributions
C) Classical signal (A+B)

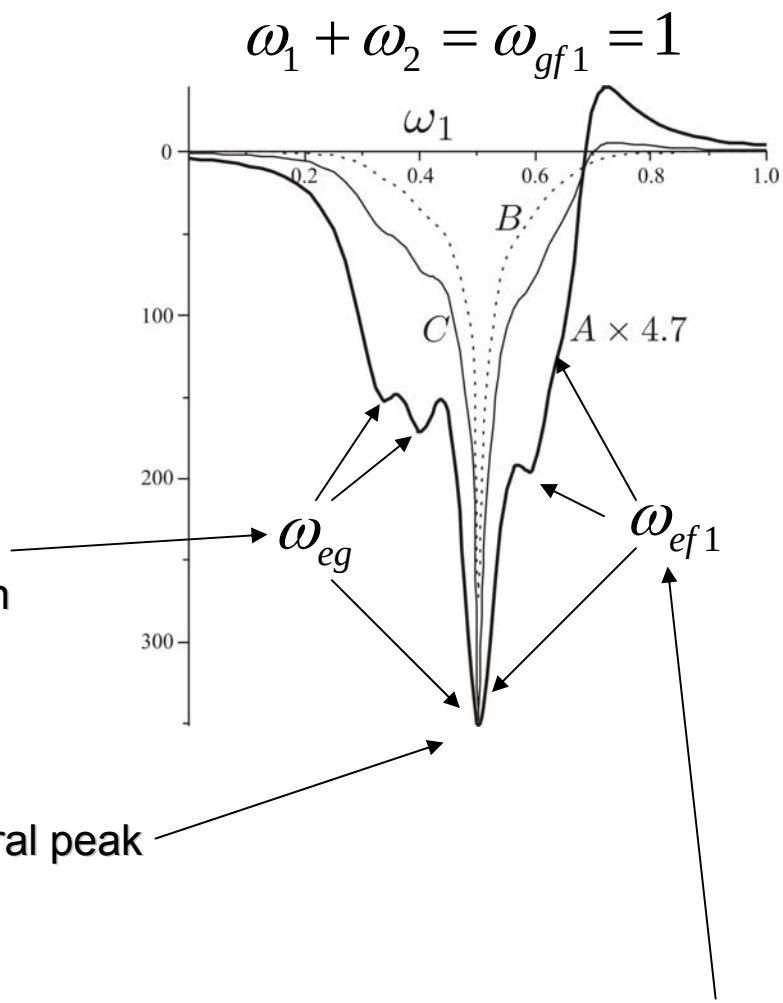

Resonances are very sensitive to the overlap between pathways due to destructive interference between pathway *iii* and pathways of group B.

Pathways *ii* and *iv* augment the central peak

The resonances are given by pathway *i* and interfere constructively with group B. They disappear slowly with Increasing dephasing.

UCIrvine
University of California, Irvine

Classical vs. entangled (PDC/MZI) signals

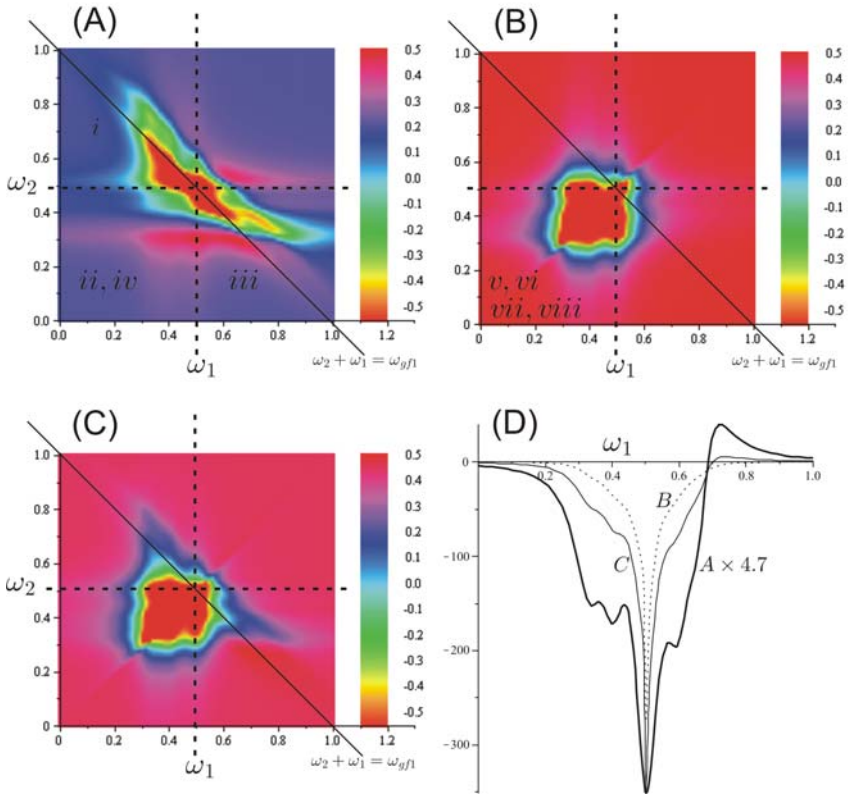

Classical signal:

1) Scales as intensity square

$$S^{(C)}(\omega_1,\omega_2) \sim |\mathrm{E}_1|^2 |\mathrm{E}_2|^2$$

2) Pathway selectivity: NO

$$S^{(C)}(\omega_1,\omega_2) \sim \Im[\chi_A^{(3)} + \chi_B^{(3)}]$$

Entangled photons signal:

1) Scales linearly with intensity:

$$S^{(C)}(\omega_1,\omega_2) \sim |\mathrm{E}_p|^2$$

2) Pathway selectivity: YES

$$S^{(C)}(\omega_1,\omega_2) \sim \Im\chi_A^{(3)}$$

UCIrvine
University of California, Irvine

TPA on a closed-time path loop.

Detector d_1 measures change in intensity of the H polarized mode $\mathbf{k}_1$ with and without (place V polarizer before the sample) mode $\mathbf{k}_2$.

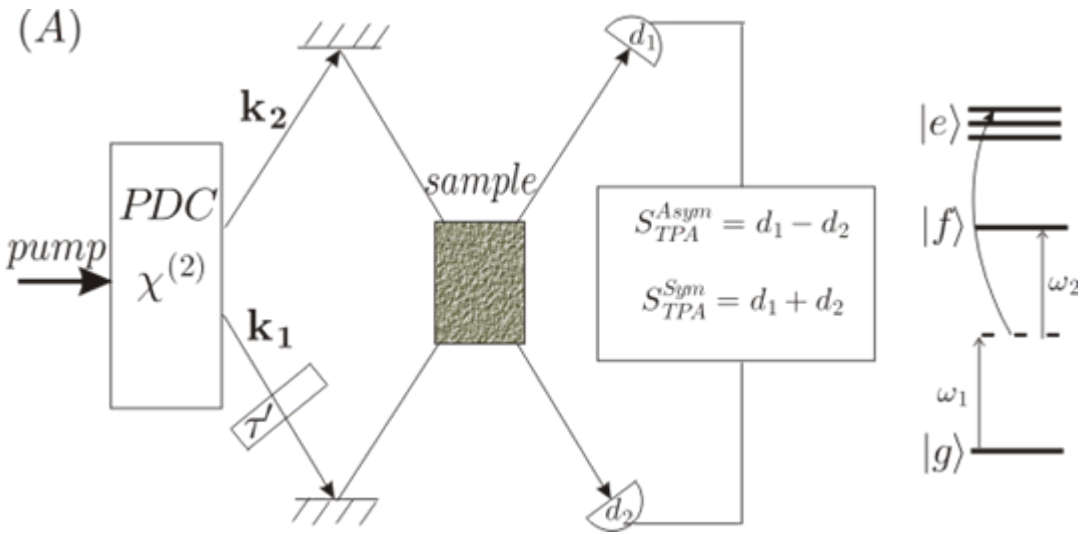

The two signals are blended together.
+ is for symmetric TPA
- is for asymmetric TPA

Detector d_2 measures change in intensity of the V polarized mode $\mathbf{k}_2$ with and without (place H polarizer before the sample) mode $\mathbf{k}_1$.

PP on a closed-time path loop.

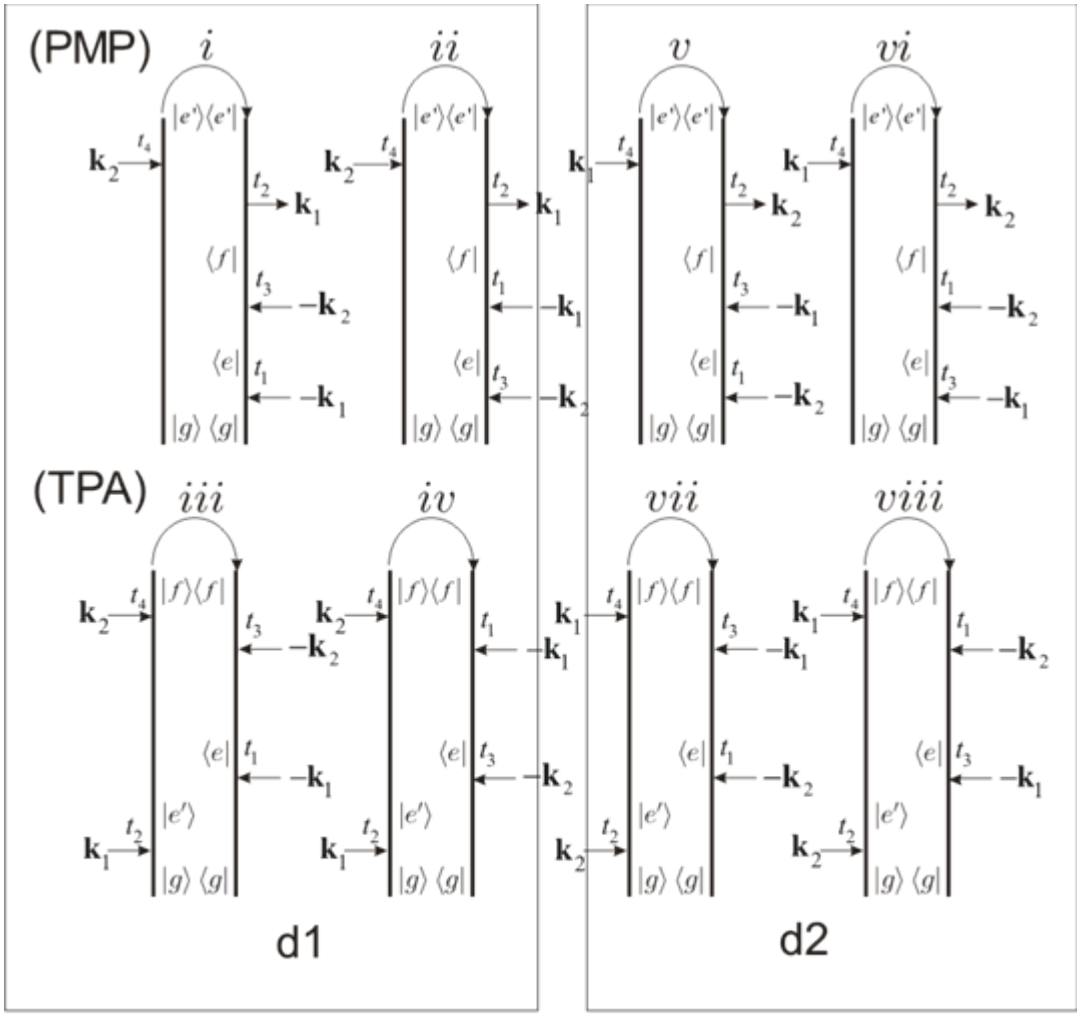

PMP - Pump modulated Probe;
TPA - Two photon absorption;
Pump-Probe symmetric = PMP +TPA =d1+d2

PP on a closed-time path loop.

PMP TPA

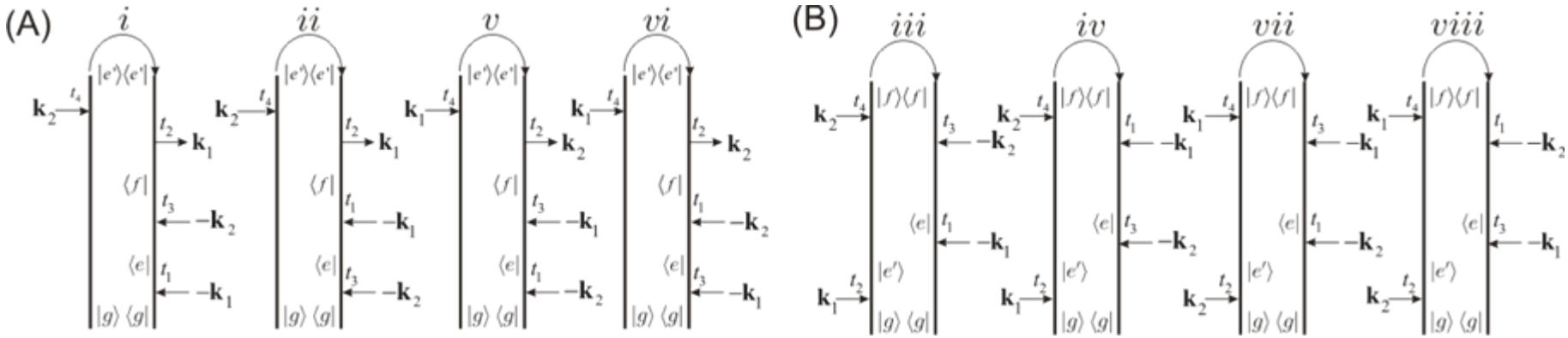

Using the loop diagrams the PP signal can be written as:

$$S_{PP}^{Sym}(\omega_1,\omega_2)=\frac{2N\pi}{\Omega}\frac{1}{2T}\int_{-T}^{T}dt_4\,\Im\frac{i^3}{3!}\int_{-\infty}^{\infty}\int_{-\infty}^{\infty}\int_{-\infty}^{\infty}dt_3dt_2dt_1$$

$$\begin{aligned}
i\quad & [\theta(t_4t_2)\theta(t_2t_3)\theta(t_3t_1)\langle V(t_1)V(t_3)V^{\dagger}(t_2)V^{\dagger}(t_4)\rangle\langle E_1^{\dagger}(t_1)E_2^{\dagger}(t_3)E_1(t_2)E_2(t_4)\rangle+\\
ii\quad & +\theta(t_4t_2)\theta(t_2t_1)\theta(t_1t_3)\langle V(t_3)V(t_1)V^{\dagger}(t_2)V^{\dagger}(t_4)\rangle\langle E_2^{\dagger}(t_3)E_1^{\dagger}(t_1)E_1(t_2)E_2(t_4)\rangle+\\
iii\quad & +\theta(t_4t_2)\theta(t_4t_3)\theta(t_3t_1)\langle V(t_1)V(t_3)V^{\dagger}(t_4)V^{\dagger}(t_2)\rangle\langle E_1^{\dagger}(t_1)E_2^{\dagger}(t_3)E_2(t_4)E_1(t_2)\rangle+\\
iv\quad & +\theta(t_4t_2)\theta(t_4t_1)\theta(t_1t_3)\langle V(t_3)V(t_1)V^{\dagger}(t_4)V^{\dagger}(t_2)\rangle\langle E_2^{\dagger}(t_3)E_1^{\dagger}(t_1)E_2(t_4)E_1(t_2)\rangle+\\
& +\{\mathbf{k}_1\leftrightarrow\mathbf{k}_2\}]
\end{aligned}$$

$v, vi, vii, viii$

PP with classical fields.

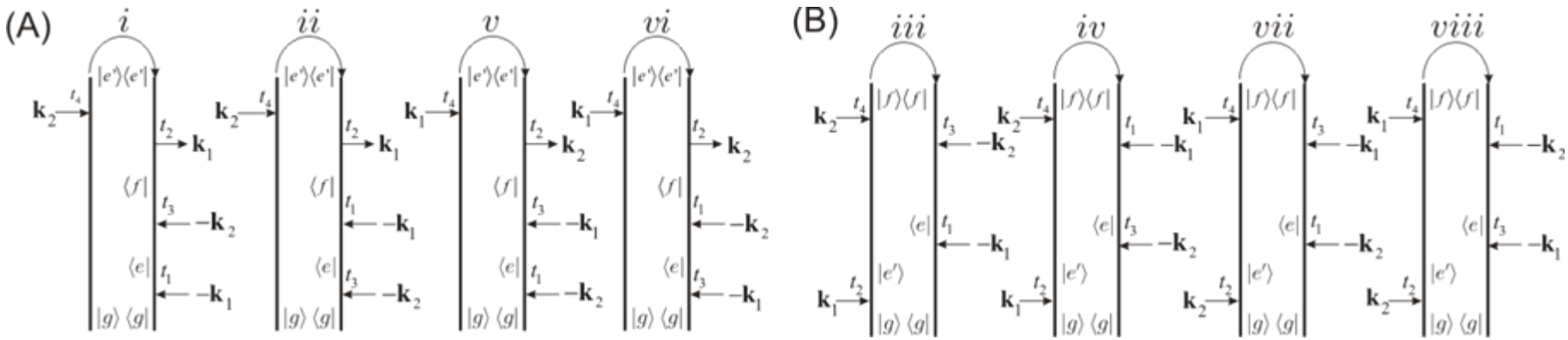

All optical field correlation functions become the product of the fields intensities:

$\langle E^{\dagger}E^{\dagger}EE\rangle = |\mathrm{E}_1|^2 |\mathrm{E}_2|^2$

At this point let us introduce the TP operator in the frequency domain:

$\mathrm{T}(\omega_1,\omega_2) = \left(V+V^{\dagger}\right)\left(G(\omega_1+\omega_g)+G(\omega_2+\omega_g)\right)\left(V+V^{\dagger}\right)$

is the Fourier transform of the retarded Green's function operator:

$$G(\omega) = -i\int_{-\infty}^{\infty} dt\theta(\tau)\exp(-iH_0\tau)e^{i\omega\tau}$$

PP with classical fields.

In the molecular eigenstates basis the only non-zero matrix elements of the TP operators (TP amplitudes) are:

$$\langle f \,|\, \mathrm{T}(\omega_1,\omega_2) \,|\, g\rangle = \mathrm{T}_{fg}(\omega_1,\omega_2) = \mu^{å}_{fe} I_{eg}(\omega_1)\mu^{å}_{eg} + \mu^{å}_{fe} I_{eg}(\omega_2)\mu^{å}_{eg}$$

$$\langle f \,|\, \mathrm{T}^{\dagger}(\omega_1,\omega_2) \,|\, g\rangle = \mathrm{T}^{å}_{fg}(\omega_1,\omega_2) = \mu^{å}_{fe} I^{å}_{eg}(\omega_1)\mu^{å}_{eg} + \mu^{å}_{fe} I^{å}_{eg}(\omega_2)\mu^{å}_{eg}$$

$$\langle g \,|\, \mathrm{T}(\omega_1,\omega_2) \,|\, f\rangle = \mathrm{T}_{gf}(\omega_1,\omega_2) = \mu_{ge} I_{ge}(\omega_1)\mu_{ef} + \mu_{ge} I_{ge}(\omega_2)\mu_{ef}$$

$$\langle g \,|\, \mathrm{T}^{\dagger}(\omega_1,\omega_2) \,|\, f\rangle = \mathrm{T}^{å}_{gf}(\omega_1,\omega_2) = \mu_{ge} I^{å}_{ge}(\omega_1)\mu_{ef} + \mu_{ge} I^{å}_{ge}(\omega_2)\mu_{ef}$$

Here we introduce the Fourier transform of the single excited state Green's function:

$$I_{eg}(\omega) = -i\int_{-\infty}^{\infty} G_{ee}(\tau)\exp(i(\omega+\omega_g)\tau)d\tau = \frac{1}{\omega-\omega_{eg}+i\gamma_{ge}}$$

γ_{ge} is the de-phasing rate;

$\exp(i\omega_g\tau)$ describes the free propagation of the molecule ground state

TPA pathways (group B).

Accompanied by emmision from state $\left| f \right\rangle$

$T_{fg}(\omega_1, \omega_2)$ absorption on the left branch (forward time) with retarded Green's functions

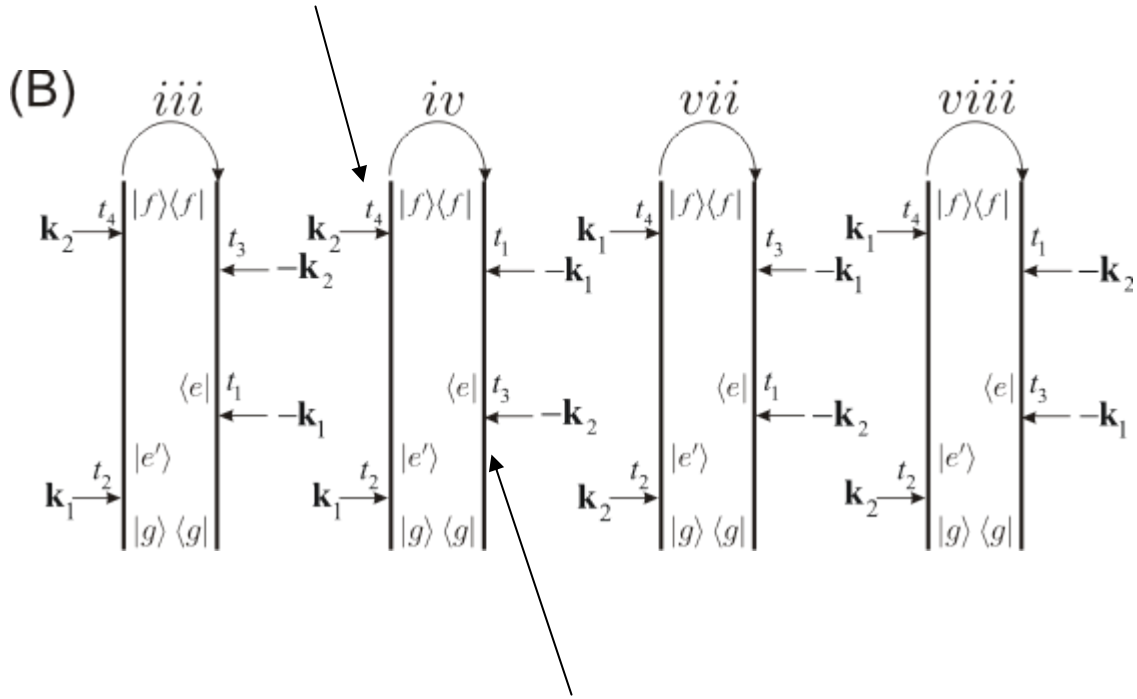

$T^{å}_{gf}(\omega_1, \omega_2)$ emission on the right branch (backward time) with advanced Green's functions

PMP pathways (group A).

Accompanied by emmision from state $|e\rangle$

$T^{\text{å}}_{fg}(\omega_1, \omega_2)$ absorption on the right branch (backward time) with advanced Green's functions

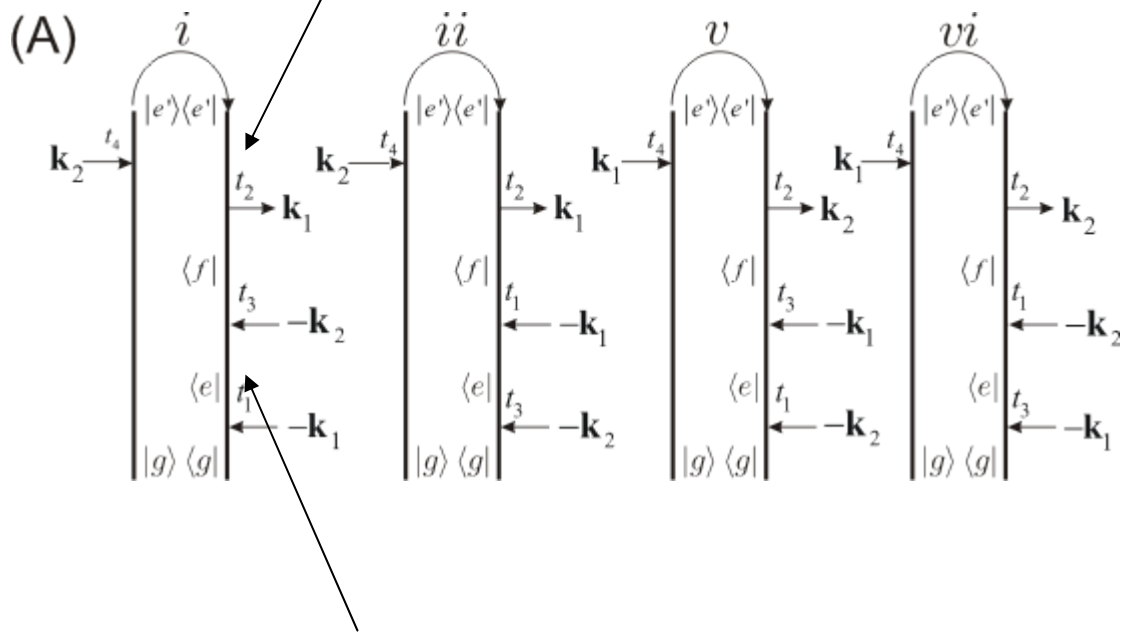

$T^{\text{å}}_{gf}(\omega_1, \omega_2)$ emission on the right branch (backward time) with advanced Green's functions

PP classical signal.

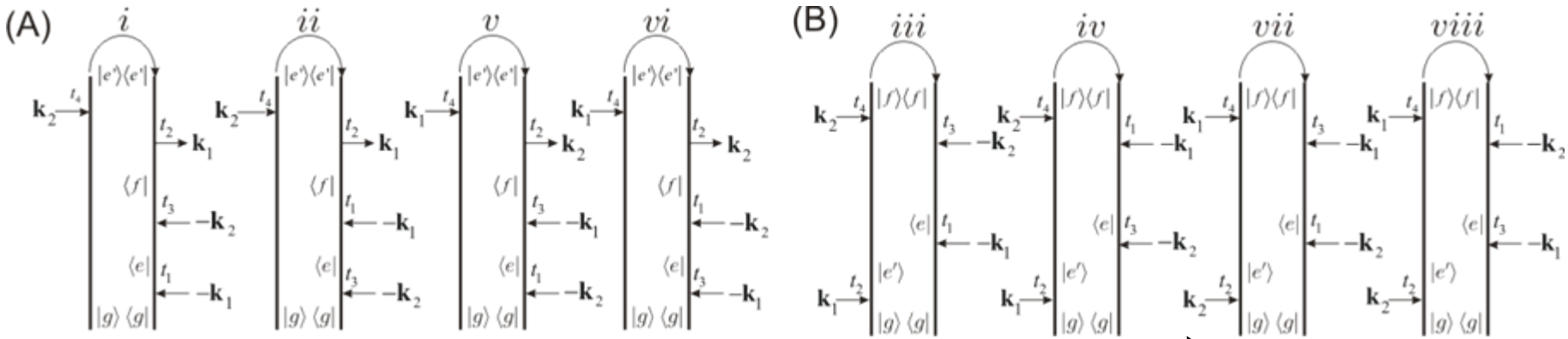

$$S_{PP}^{Sym}(\omega_1,\omega_2) = -\frac{2\pi N\,|\,\mathrm{E}_1\,|^2\,|\,\mathrm{E}_2\,|^2}{3!\Omega}\,\Im I_{fg}^{\text{å}}(\omega_1+\omega_2)\left[T_{fg}^{\text{å}}(\omega_1,\omega_2)\mathrm{T}_{gf}^{\text{å}}(\omega_1,\omega_2)+\mathrm{T}_{fg}(\omega_1,\omega_2)\mathrm{T}_{gf}^{\text{å}}(\omega_1,\omega_2)\right]$$

The system evolution after the two photons had been absorbed is described by the double excited state Green's function

$$I_{fg}(\omega) = \frac{1}{\omega-\omega_{fg}+i\gamma_{fg}}$$

For off-resonant single excited state $\mathrm{T}_{fg}(\omega_1,\omega_2)\mathrm{T}_{gf}^{\text{å}}(\omega_1,\omega_2) = \mathrm{T}_{fg}^{\text{å}}(\omega_1,\omega_2)\mathrm{T}_{gf}^{\text{å}}(\omega_1,\omega_2)$

and the signal is : $\delta\left(\omega_1+\omega_2-\omega_{fg}\right)|\,\mathrm{T}_{fg}(\omega_1,\omega_2)\,|^2$

Twin state as initial state of the field.

Twin state is defined as:

$$|\psi\rangle = C\sum_{\mathbf{k}_1}\sum_{\mathbf{k}_2} t_I \exp\left(-i\frac{\Delta\omega t_I}{2}\right)\mathrm{sinc}\left(\frac{\Delta\omega t_I}{2}\right)\exp\left(-i\frac{(\Delta\mathbf{k})_z L_z}{2}\right)\mathrm{sinc}\left(\frac{(\Delta\mathbf{k})_z L_z}{2}\right)|\mathbf{k}_1,\mathbf{k}_2\rangle$$

Here $\Delta\omega = \omega_p - \omega_1 - \omega_2, \Delta\mathbf{k} = \mathbf{k}_p - \mathbf{k}_1 - \mathbf{k}_2,$

t_I is the interaction time within the PDC crystal of width L_z.

The normalization constant $C = \chi^{(2)}\mathrm{E}_p / \sqrt{A_{12}}$ is proportional to

the nonlinearity of the PDC crystal $\chi^{(2)}$, the pump electric field amplitude E_p

and the entanglement area A_{12}.

The Fock state $|\mathbf{k}_1,\mathbf{k}_2\rangle$ contains one photon in each mode $\mathbf{k}_1$ and $\mathbf{k}_2$.

Twin state (no delay) correlation functions.

For the twin states the optical field correlation functions $\langle E^{\dagger}E^{\dagger}EE\rangle$ are factorized into the products of the field transition amplitudes:

$$\langle 0,0 \mid E_2(t_4)E_1(t_2) \mid \psi\rangle = \theta(t_4 t_2)F(t_4,t_2,T_{12}) + \theta(t_2 t_4)F(t_2,t_4,T_{12}) =$$
$$\langle \psi \mid E_1^{\dagger}(t_3)E_2^{\dagger}(t_1) \mid 0,0\rangle = \theta(t_3 t_1)F^{\text{å}}(t_3,t_1,T_{12}) + \theta(t_1 t_3)F^{\text{å}}(t_1,t_3,T_{12}) =$$

$$F(t_4,t_2,T_{12}) = \frac{2\pi\chi^{(2)}\mathrm{E}_p}{\Omega}\sqrt{\frac{\omega_1\omega_2}{A_{12}T_{12}}}\exp\left(-i(\omega_1 t_2 + \omega_2 t_4)\right)\mathrm{rect}\left(\frac{t_4 - t_2}{T_{12}}\right)$$

where rect(t) is the rectangular function equal to 1 for $0 \le t \le 1$ and 0 otherwise.

Twin state (no delay) correlation functions.

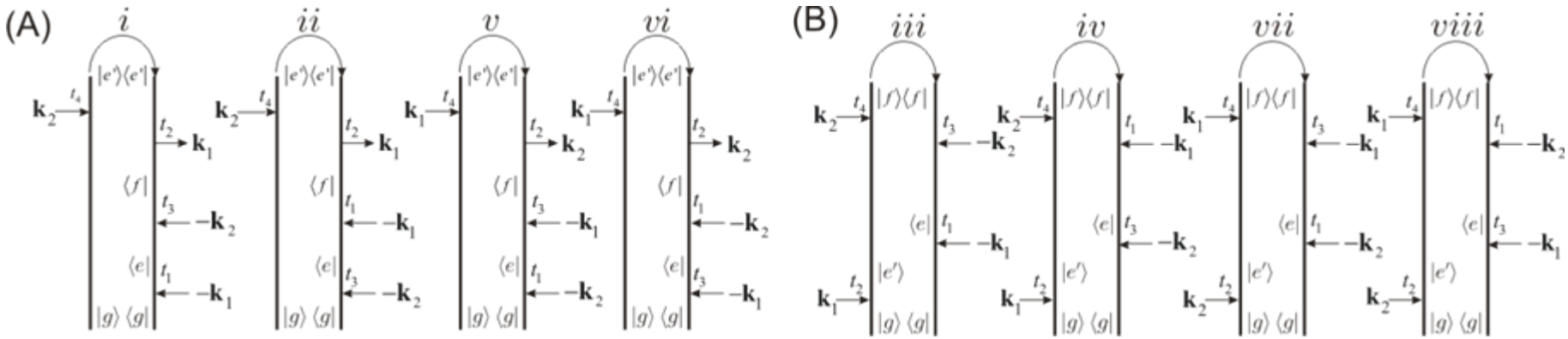

The signal becomes:

$$S_{PP}^{Sym}(\omega_1,\omega_2)=\frac{2N\pi}{\Omega}\frac{1}{2T}\int_{-T}^{T}dt_4\,\Im\frac{i^3}{3!}\int_{-\infty}^{\infty}\int_{-\infty}^{\infty}\int_{-\infty}^{\infty}dt_3dt_2dt_1$$

$$[\theta(t_4t_2)\theta(t_2t_3)\theta(t_3t_1)\langle V(t_1)V(t_3)V^{\dagger}(t_2)V^{\dagger}(t_4)\rangle F^{å}(t_3,t_1,T_{12})F(t_4,t_2,T_{12})+$$
$$+\theta(t_4t_2)\theta(t_2t_1)\theta(t_1t_3)\langle V(t_3)V(t_1)V^{\dagger}(t_2)V^{\dagger}(t_4)\rangle F^{å}(t_1,t_3,T_{12})F(t_4,t_2,T_{12})+$$
$$+\theta(t_4t_2)\theta(t_4t_3)\theta(t_3t_1)\langle V^1(t_1)V^2(t_3)V^{\dagger}(t_4)V^{\dagger}(t_2)\rangle F^{å}(t_3,t_1,T_{12})F(t_2,t_4,T_{12})+$$
$$+\theta(t_4t_2)\theta(t_4t_1)\theta(t_1t_3)\langle V^2(t_3)V^1(t_1)V^{\dagger}(t_4)V^{\dagger}(t_2)\rangle F^{å}(t_1,t_3,T_{12})F(t_2,t_4,T_{12})+$$
$$+\{\mathbf{k}_1\leftrightarrow\mathbf{k}_2\}]$$

Twin state (no delay) TP transition amplitudes.

At this point let us introduce the following transformation of the material Green's function $G_{eg}(\tau)$ due to the entanglement between the photons:

$$J_{eg}(\omega,T_{12}) = \int_{-\infty}^{\infty} G_{ee}(\tau)\mathrm{rect}(\frac{\tau}{T_{12}})\exp(i\omega\tau)d\tau = \frac{e^{i(\omega-\omega_{eg}+i\gamma_{eg})T_{12}}-1}{\omega-\omega_{eg}+i\gamma_{eg}}$$

That is the role of the entanglement is the modification of the Fourier transformation of the material Green's function. $J_{eg}(\omega,T_{12})$ can be alternatively viewed as the Fourier transformation of the joined matter/entangled photon Green's function.

Modified TP transition amplitude is:

$$\mathrm{T}_{fg}(\omega_1,\omega_2,T_{12}) = \mu_{ge}\mu_{ef}J_{eg}(\omega_1,T_{12}) + \mu_{ge}\mu_{ef}J_{eg}(\omega_2,T_{12})$$

TP induced transparency.

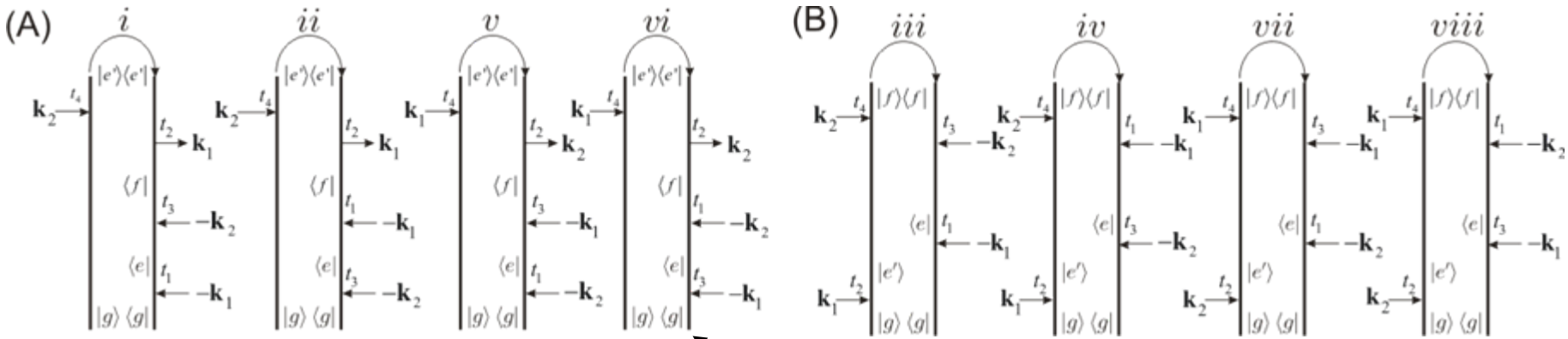

$$S_{PP}^{Sym}(\omega_1,\omega_2,T_{12}) = -\frac{(2\pi)^3 N\,|\,\chi^{(2)}\,|^2\,|\,\mathrm{E}_p\,|^2\,\omega_1\omega_2}{3!A_{12}T_{12}\Omega^3}\,\Im I_{fg}^{\text{å}}(\omega_1+\omega_2)\Big[\mathrm{T}_{fg}^{\text{å}}(\omega_1,\omega_2,T_{12})\mathrm{T}_{gf}^{\text{å}}(\omega_1,\omega_2,T_{12}) + |\,\mathrm{T}_{fg}(\omega_1,\omega_2,T_{12})\,|^2\Big]$$

CTPL correction

Glauber two-photon counting

For the off-resonant single states $\mathrm{T}_{fg}^{\text{å}}(\omega_1,\omega_2,T_{12}) \neq \mathrm{T}_{fg}(\omega_1,\omega_2,T_{12})$ and the symmetric TPA signal does not dissapear.

What is the role of $\mathrm{T}_{fg}^{\text{å}}(\omega_1,\omega_2,T_{12})\;\mathrm{T}_{gf}^{\text{å}}(\omega_1,\omega_2,T_{12})$ term?

PP entanglement time spectra

$$S^{\nu}_{PP}(\omega_p/2,\omega_T) = \mathrm{N}\int_{T_{min}}^{T_{max}} dT_{12}\exp(i\omega_{T_{12}}T_{12})S^{\nu}_{PP}(\omega_p/2,T_{12})$$

$$\nu = d_1, d_2, Sym, Asym$$

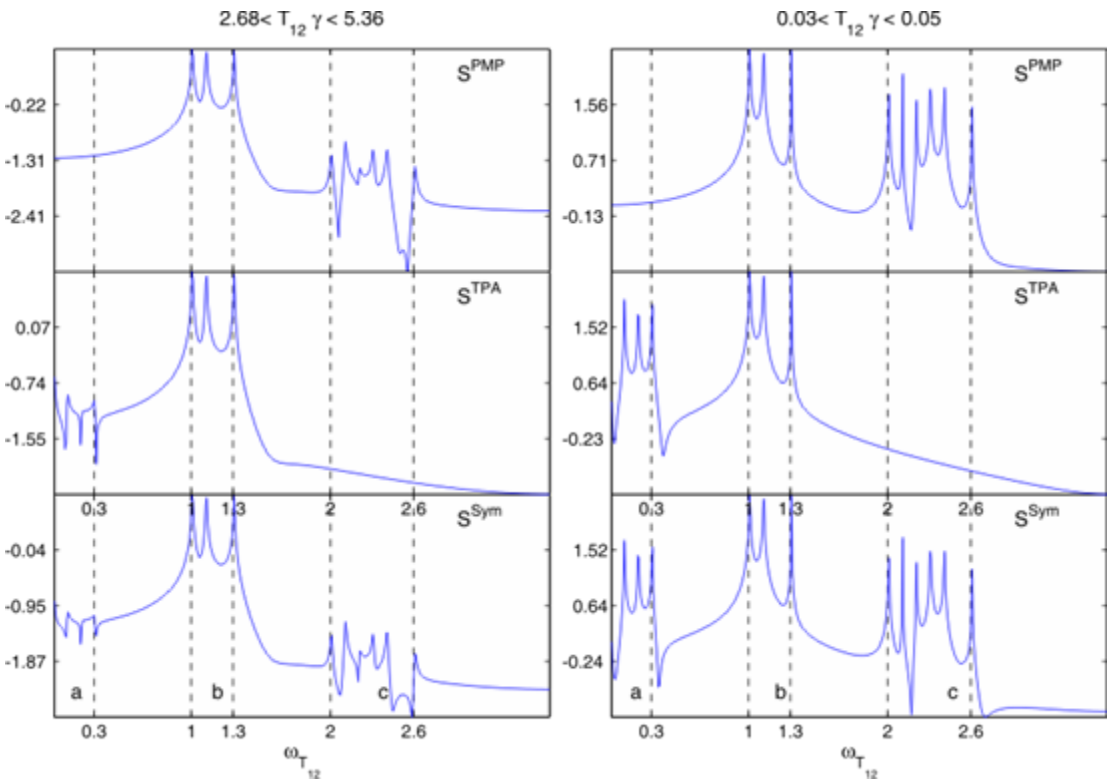

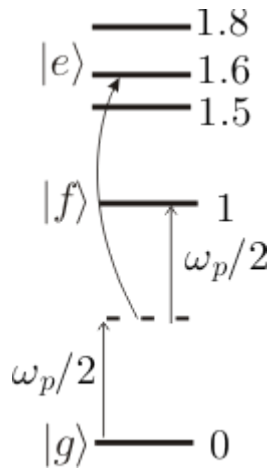

Group (a) of resonances:

$\omega_{eg} - \omega_{e'g} \in [0, 0.3]$

Group (b) of resonances:

$\omega_{eg} - \omega_p / 2 \in [1, 1.3]$

Group (c) of resonances:

$\omega_{eg} + \omega_{e'g} - \omega_p \in [2, 2.6]$

PP entanglement time spectra

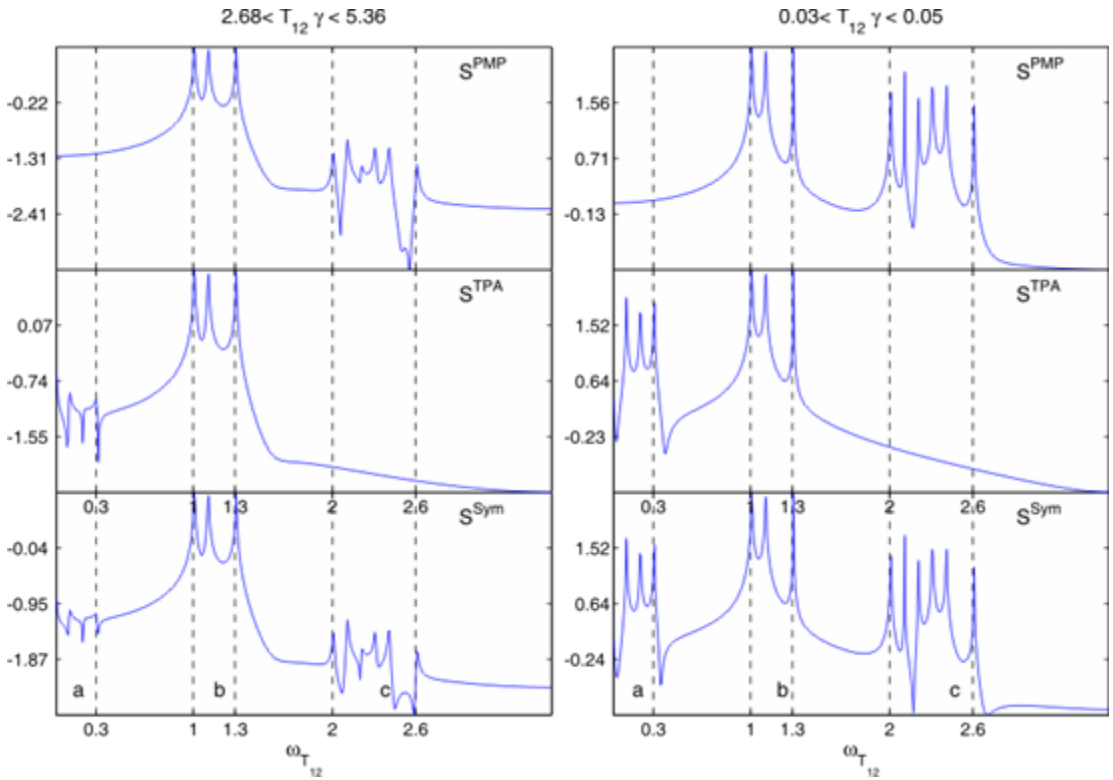

1) All pathways interfere constructively.

2) b resonances can be detected by a conventional pump-probe with short well separated pulses.

3) Increasing the dephasing rate (left column) quenches the resonances in regions a and c.

PP entanglement time spectra

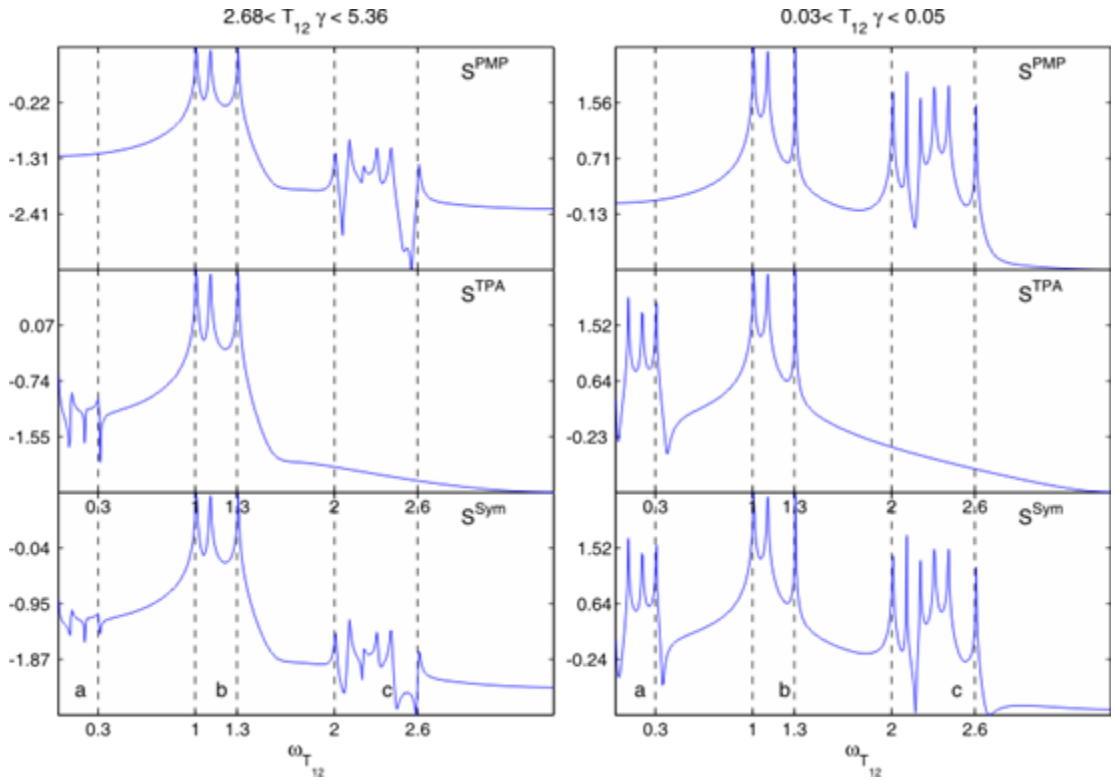

4) PMP pathways contribute to spectral regions b and c.

5) TPA pathways show resonances in regions a and b.

6) $S^{d_1} = S^{d_2} = S^{Sym}$

7) The assymertic signal vanishes.

PP with mutually delayed twin photons.

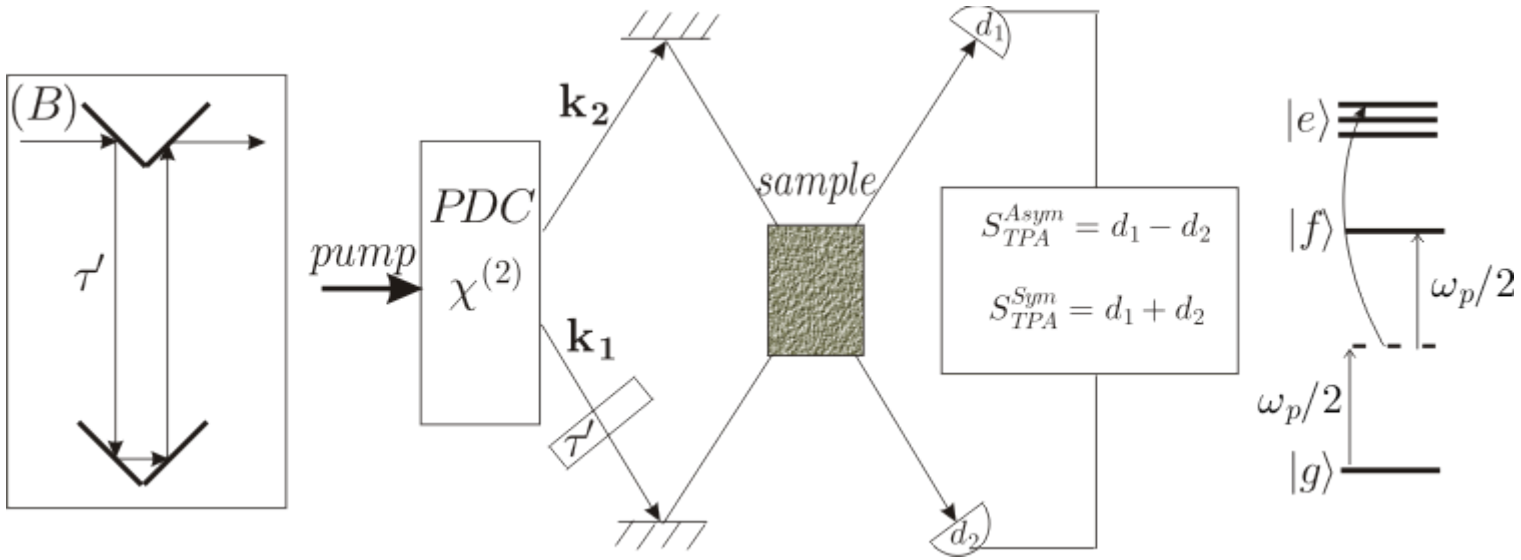

Now let us consider a different TPA setup with twin photons close to those proposed by Saleh. The frequencies of the beams are fixed to be $\omega_1 = \omega_2 = \omega_p / 2$ and we introduce a relative time delay τ' between the tween photons:

$$E_1(t) = \left(\frac{\pi \omega_p}{\Omega} \right)^{1/2} a_1 \exp(-i\omega_p (t - \tau'/2)/2)$$

$$E_2(t) = \left(\frac{\pi \omega_p}{\Omega} \right)^{1/2} a_2 \exp(-i\omega_p (t + \tau'/2)/2)$$

PP with mutually delayed twin photons. Twin correlation functions.

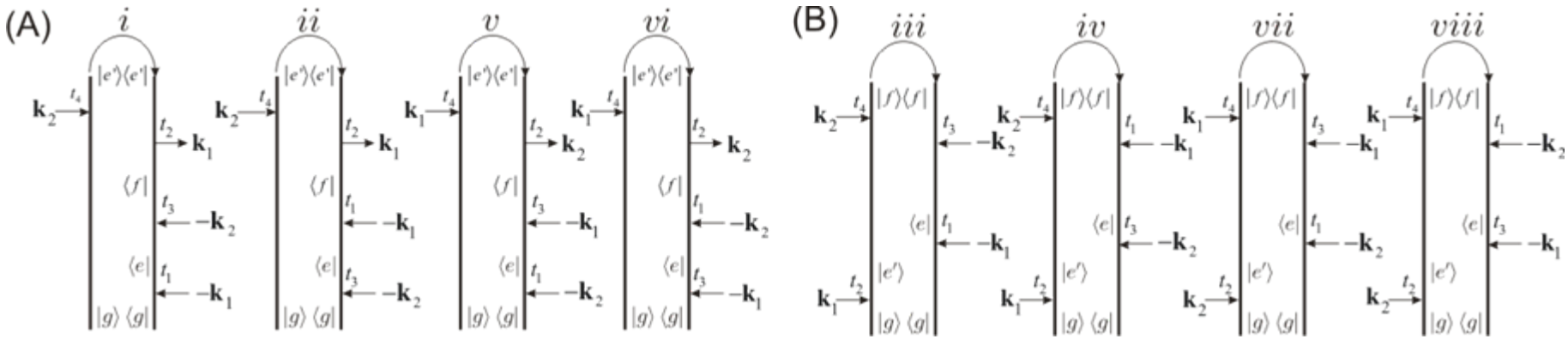

The field transformation amounts to the following TP transition amplitudes for the diagrams (i-iv):

$$\langle 0,0 \,|\, E_2(t_4)E_1(t_2) \,|\, \psi^{(2)}(0)\rangle = \theta(t_4 t_2)F(t_4,t_2,T_{12}) + \theta(t_2 t_4)F(t_2,t_4,T_{12})$$

$$\langle \psi^{(2)}(0) \,|\, E_1^{\dagger}(t_3)E_2^{\dagger}(t_1) \,|\, 0,0\rangle = \theta(t_3 t_1)F^{\text{å}}(t_3,t_1,T_{12}) + \theta(t_1 t_3)F^{\text{å}}(t_1,t_3,T_{12})$$

$$F(t_4,t_2,T_{12}) = \frac{\pi\chi^{(2)}\mathrm{E}_p\omega_p}{\Omega\sqrt{A_{12}T_{12}}}\exp\left(-i\omega_p/2(t_4+t_2)\right)\mathrm{rect}\left(\frac{t_4-t_2}{T_{12}-\tau'}\right)$$

For the diagrams (v-viii)one has to interchange $t_4 \leftrightarrow t_2, t_3 \leftrightarrow t_1$

PP with mutually delayed twin photons. Matter transition amplitudes.

$J_{eg}(\omega_p / 2, T_{12}\, \mathrm{m}\, \tau')$ describe the Fourier transform of the system(twin/matter) Green′sfunction by incorporating the relativedelay τ' between the entangled photons.

This delay breaks the symmetry of the Green's function and makes it dependent on the order in which the twins are absorbed or emitted.

If $\mathbf{k}_2$ mode precedes $\mathbf{k}_1$ the system evolves by: $\mathrm{J}_{eg}(\omega, T_{12} - \tau')$

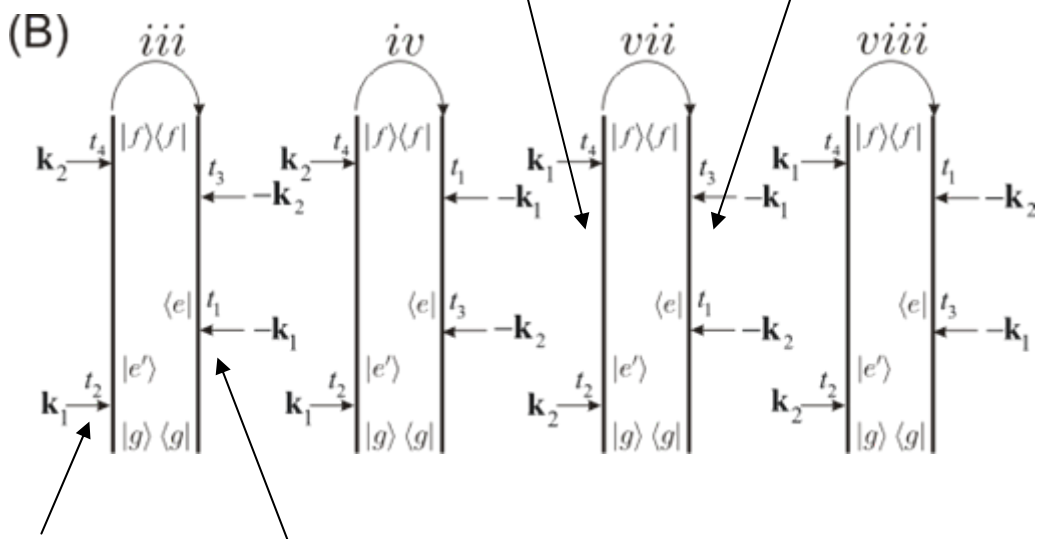

If $\mathbf{k}_1$ mode precedes $\mathbf{k}_2$ the system evolves by: $\mathrm{J}_{eg}(\omega, T_{12} - \tau')$

TPA with mutually delayed twin photons.

Using the transition amplitude above, the symmetrized signal can be rewritten as:

$$S_{TPA}^{Sym}(\omega_p/2,T_{12},\tau') = -\frac{2\pi^3 N |\chi^{(2)}|^2 |\mathrm{E}_p|^2 \omega_p^2}{3! A_{12} T_{12} \Omega^3} \Im I_{fg}^{\text{å}}(\omega_p)\left[\mathrm{T}_{fg}^{\text{å}}(\omega_p/2,T_{12},\tau')\mathrm{T}_{gf}^{\text{å}}(\omega_p/2,T_{12},\tau') + |\mathrm{T}_{fg}(\omega_p,T_{12},\tau')|^2\right]$$

So far we have considered the symmetrized TPA signal, but as an alternative one can anti-symmetrize it by monitoring the difference between the detector d_1 and d_2 :

$$S_{TPA}^{(Asym)}(\omega_p/2,T_{12},\tau') = -\frac{2\pi^3 N |\chi^{(2)}|^2 |\mathrm{E}_p|^2 \omega_p^2}{3! A_{12} T_{12} \Omega^3} \Im I_{fg}^{\text{å}}(\omega_p)\times$$

$$\left[\mathrm{T}_{gf}^{\text{å},+}(\omega_p/2,T_{12},\tau')\mathrm{T}_{gf}^{\text{å},-}(\omega_p/2,T_{12},\tau') + \mathrm{T}_{gf}^{-}(\omega_p/2,T_{12},\tau')(\mathrm{T}_{fg}^{+}(\omega_p/2,T_{12},\tau'))^{\text{å}}\right]$$

Here we introduced the symmetric (+) and anti-symmetric (-) TP transition amplitudes:

$$\mathrm{T}_{gf}^{+}(\omega_p/2,T_{12},\tau') = \mu_{ge}\mu_{ef} I_{eg}(\omega_p/2,T_{12}-\tau') + \mu_{ge}\mu_{ef} I_{eg}(\omega_p/2,T_{12}+\tau')$$

$$\mathrm{T}_{gf}^{-}(\omega_p/2,T_{12},\tau') = \mu_{ge}\mu_{ef} I_{eg}(\omega_p/2,T_{12}-\tau') - \mu_{ge}\mu_{ef} I_{eg}(\omega_p/2,T_{12}+\tau')$$

The asymmetric TPA signal vanishes in absense of the delay $\tau' = 0$.

PP delay time spectra

$$S^{\nu}_{PP}(\omega_p/2, T_{12}, \omega_\tau) = \mathrm{N} \int_0^{T_{12}} d\tau \exp(i\omega_\tau \tau) S^{\nu}_{PP}(\omega_p/2, T_{12}, \tau)$$

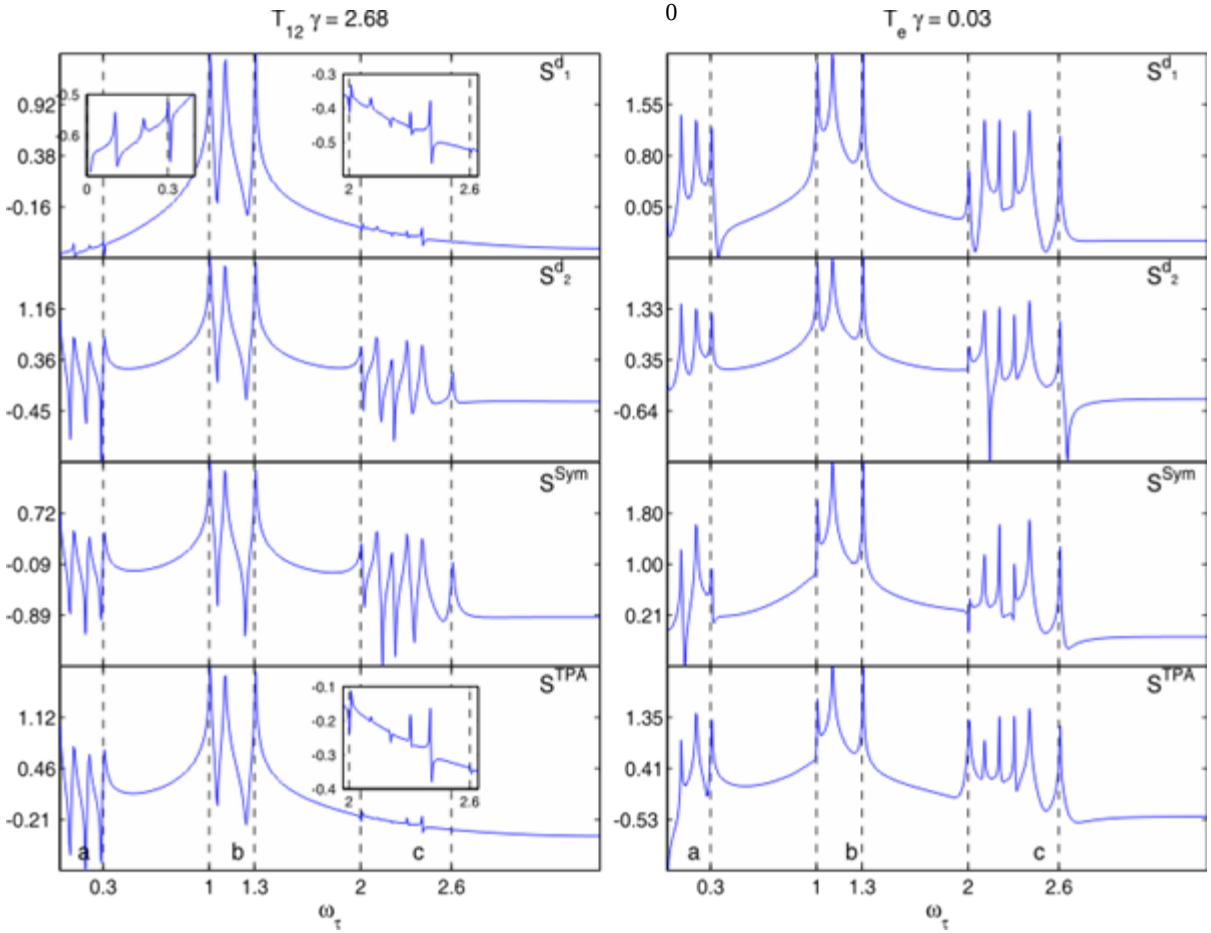

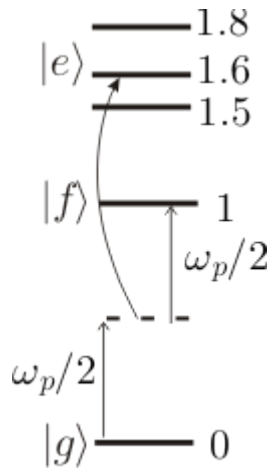

Group (a) of resonances:

$\omega_{eg} - \omega_{e'g} \in [0, 0.3]$

Group (b) of resonances:

$\omega_{eg} - \omega_p / 2 \in [1, 1.3]$

Group (c) of resonances:

$\omega_{eg} + \omega_{e'g} - \omega_p \in [2, 2.6]$

PP delay time spectra

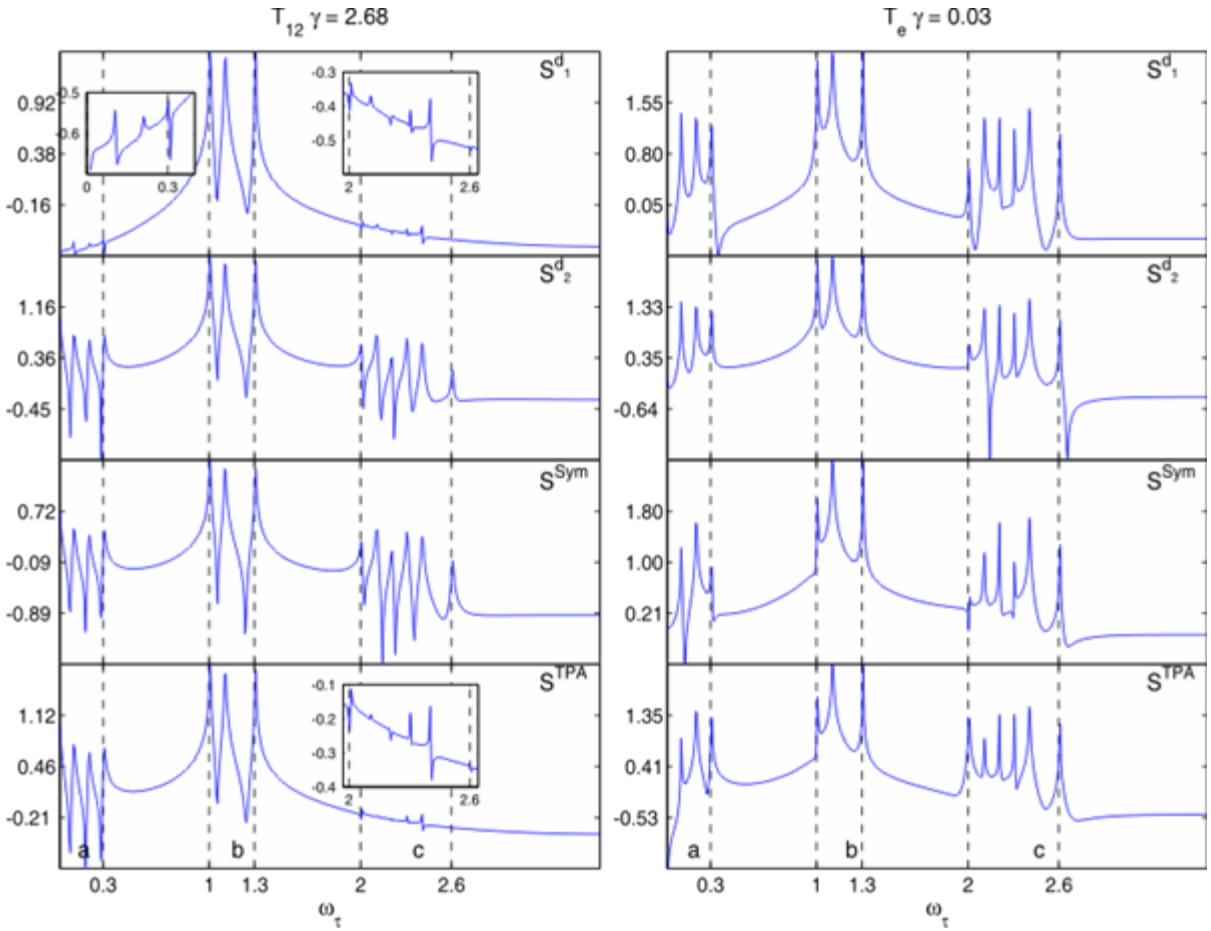

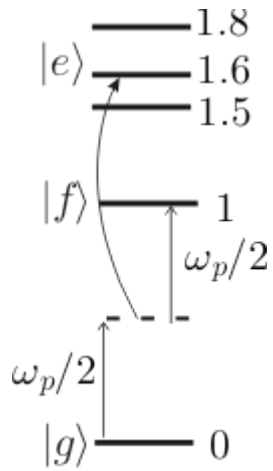

In numerical simulations we assume that we can increase the time delay with a step $\Delta\tau \le 2\pi / (\max(\omega_{eg} + \omega_{e'g} - \omega_p) = 0.025$ up to the value of the entanglement time $T_{12} = 2^{10}\Delta\tau.$

If the unit of energy is $1\mathrm{Ev}$ then the step is $\Delta\tau' = 1.3\mathrm{fs}.$

PP delay time spectra

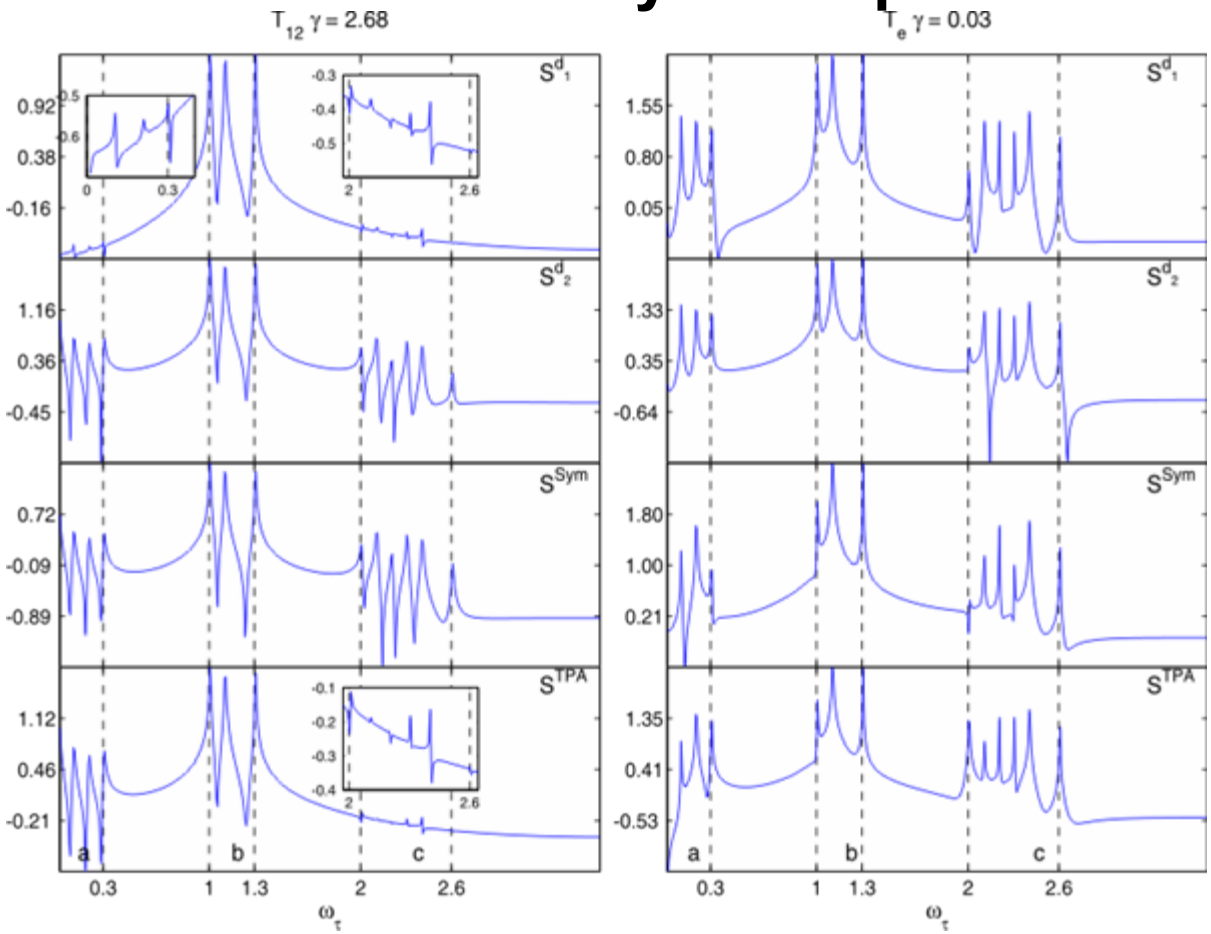

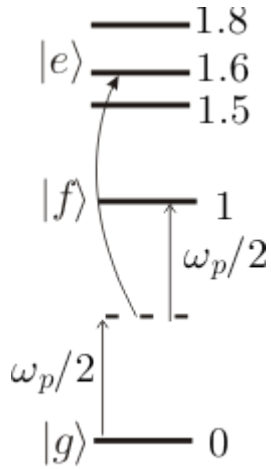

For PMP (TPA) pathways region a (c) resonances are produced by the pathways i,v,iii,vii where emitted and absorbed photon follow the same chronological order; the region c (a) resonances are given by the pathways ii,vi,iv,viii where the chronological photon order for the emission is opposite to those of the absorption. This peculiar feature is a result of broken symmetry of the field transition amplitude.

PP delay time spectra

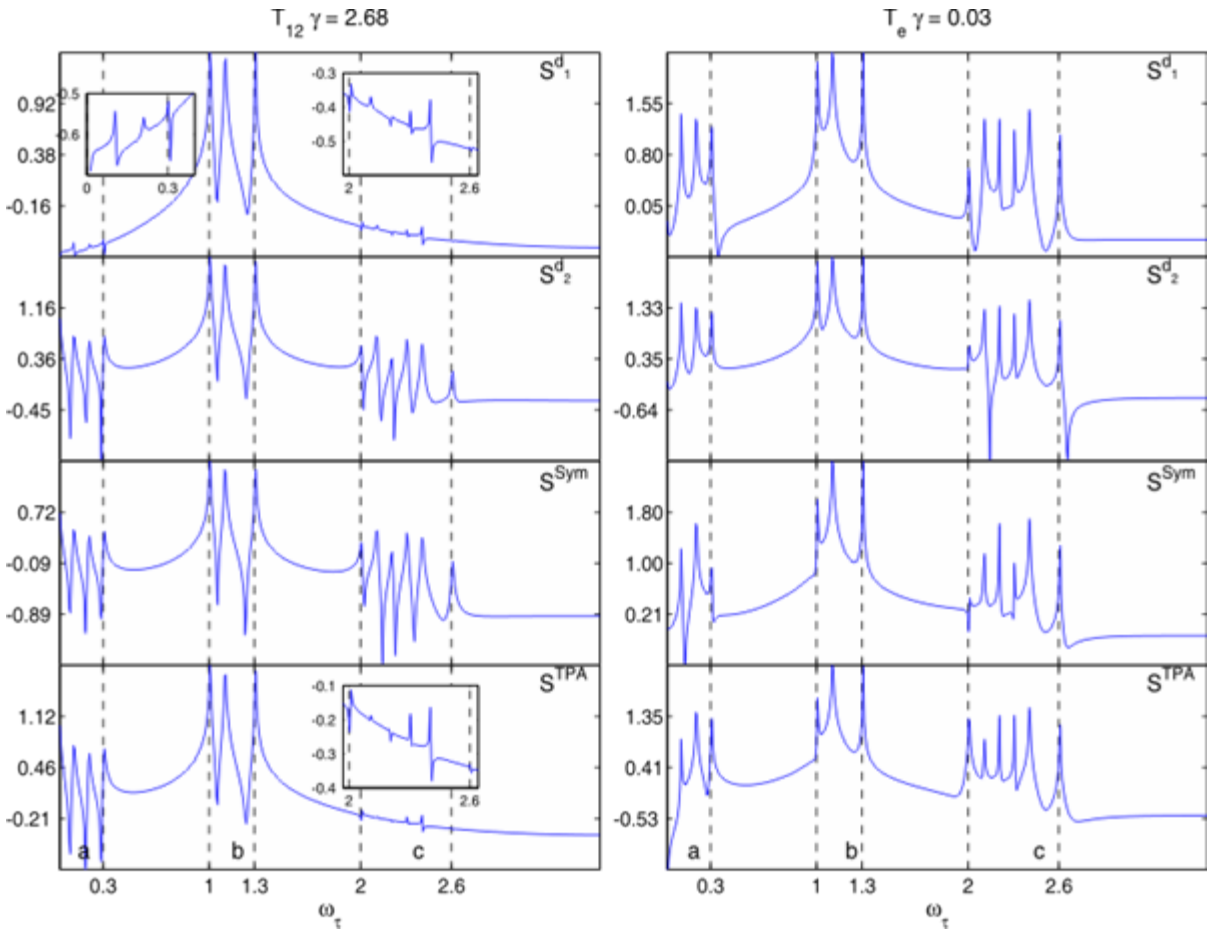

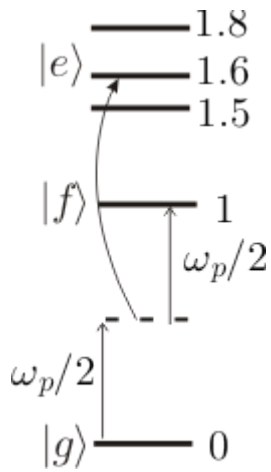

1) For small dephasing rate (right panle) PMP and TPA contribute to the same regions in all spectra and spectrally non separable by the pump-probe technique.

2) At large dephasing rate (left panel) pathways v-viii do not contribute regions a and c.

PP delay time spectra

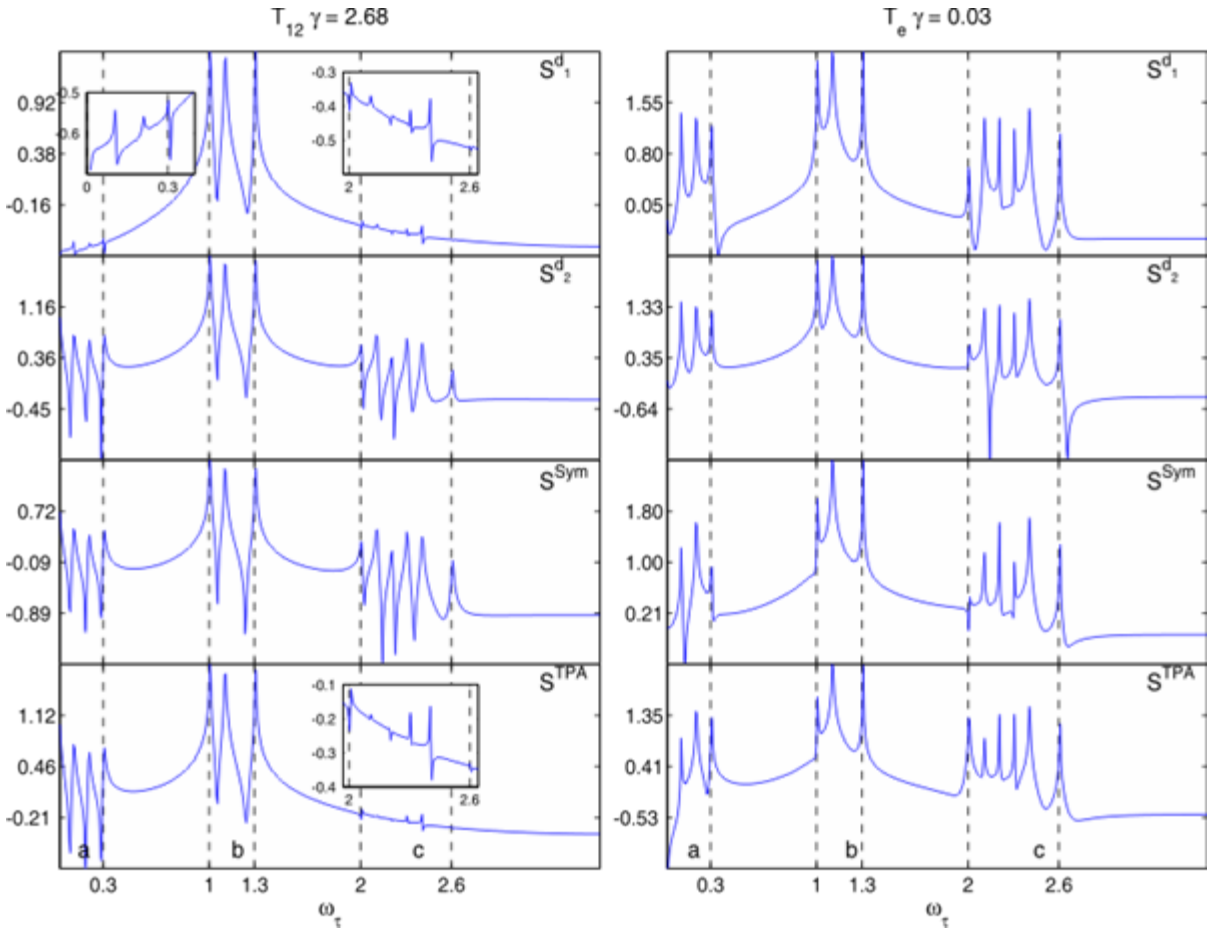

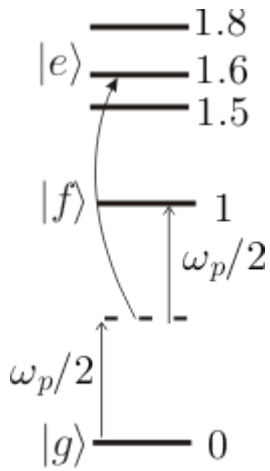

3) The spectra obtained from the two detectors are different.

4) Only the S^{d_2} signal reveals the resonances in the non-classical regions a and c.

5) Both S^{Sym} and S^{Asym} signals contain all resonances.

6) The TPA signal misses the region c resonances, and PMP misses resonances in region a, thus one can separate PMP from TPA if focuses on the regions a and c only.

PP correlation spectra. Detector 1 and 2.

$$S^{\nu}_{TPA}(\omega_p/2,\omega_{T_{12}},\omega_\tau) = \mathrm{N}\int_{T_{min}}^{T_{max}} dT_{12}\exp(i\omega_{T_{12}}T_{12})\int_{0}^{T12} d\tau\exp(i\omega_\tau\tau)S^{\nu}_{TPA}(\omega_p/2,T_{12},\tau)$$

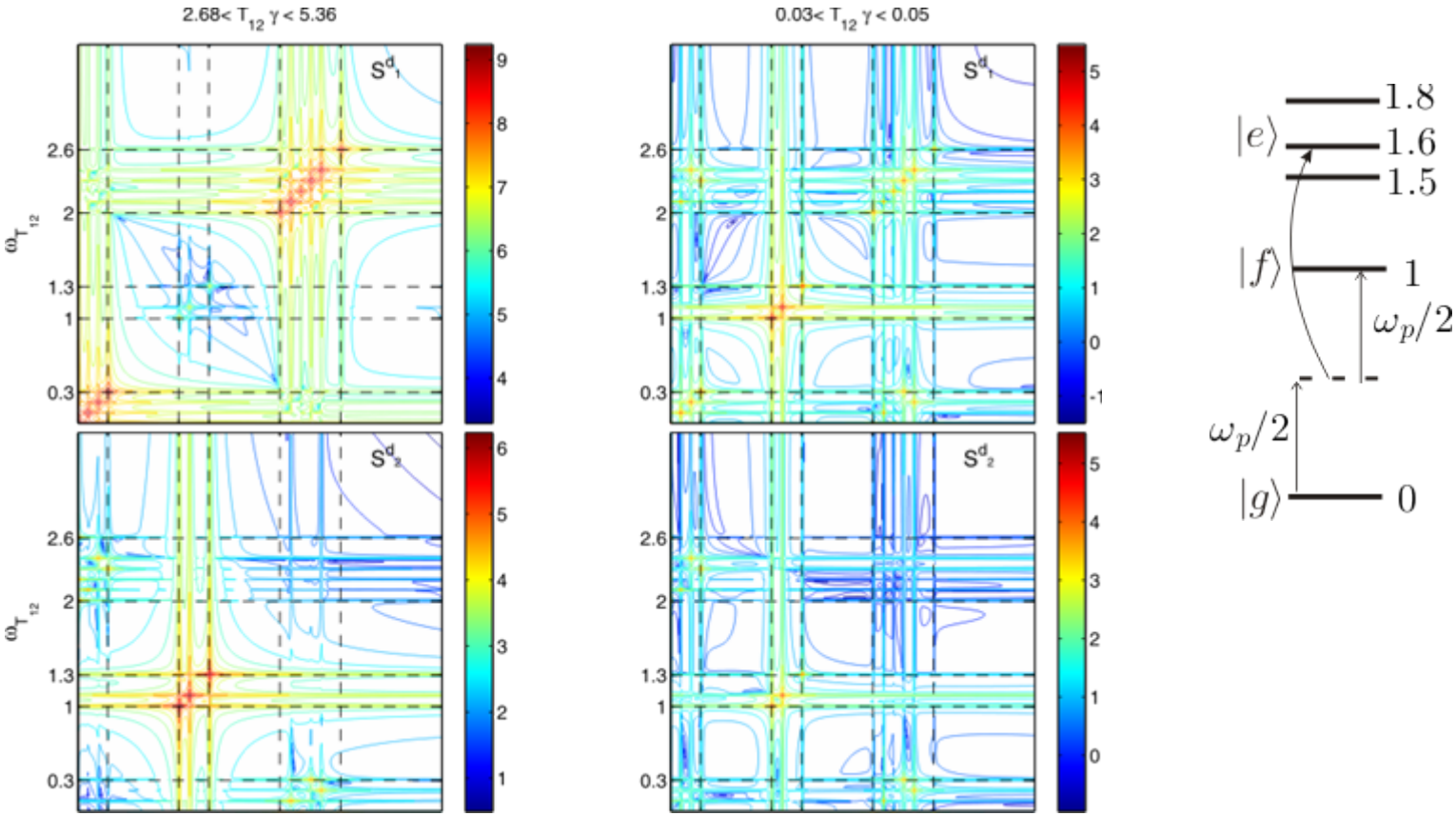

The correlation spectra from the two detectors are different. Unlike the delay spectra, detector d1 reveals all spectral regions, while resonances (a,a) and (c,c) from detector d2 are suppressed.

PP correlation spectra. TPA and Sym spectra.

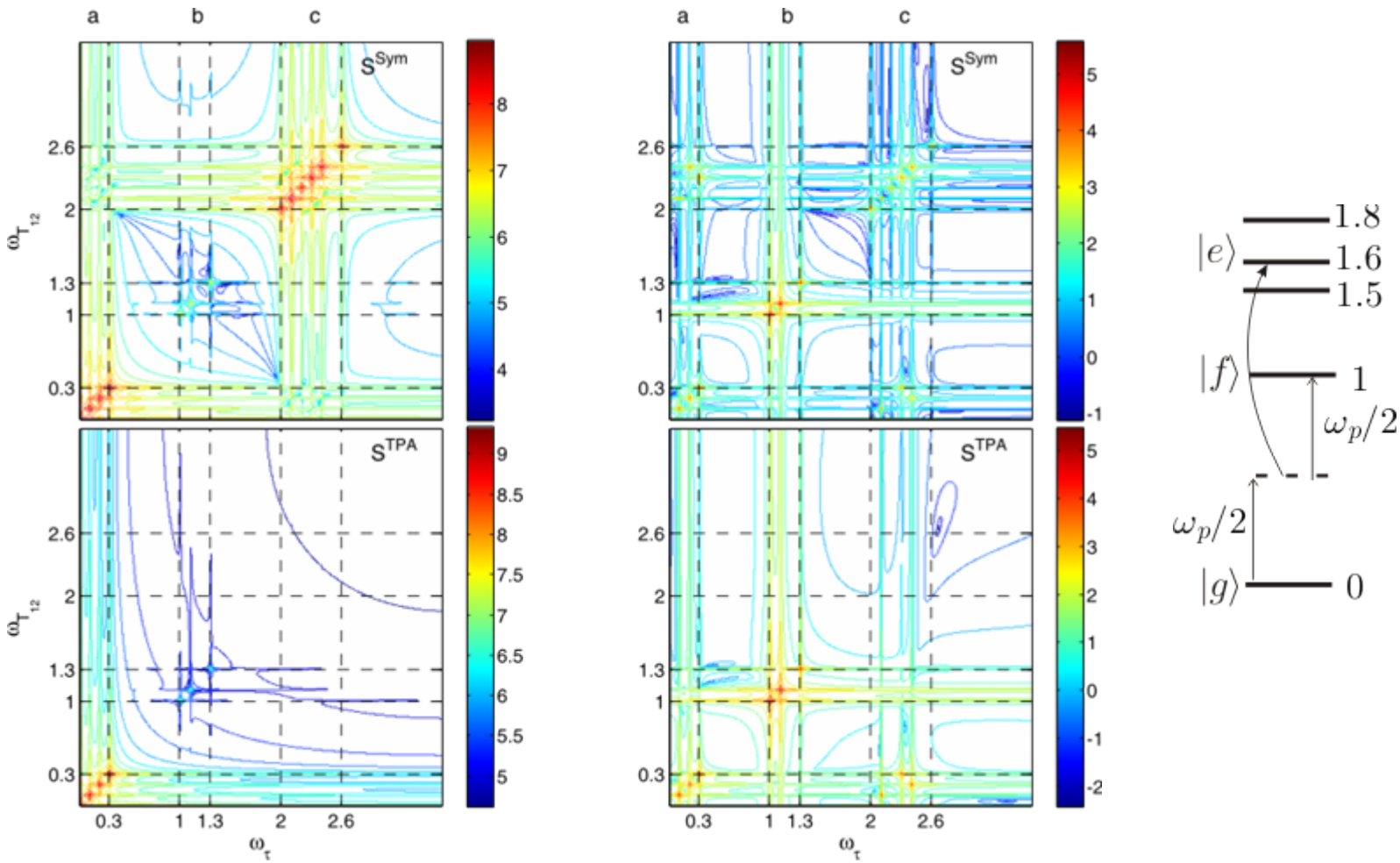

1) The off-diagonal, as well as (b,b), resonances are sensitive to the dephasing rate and vanish for large dephasing. The diagonal (a,a) and (c,c) resonances overlap as the dephasing rate increases.

PP correlation spectra. TPA and Sym spectra.

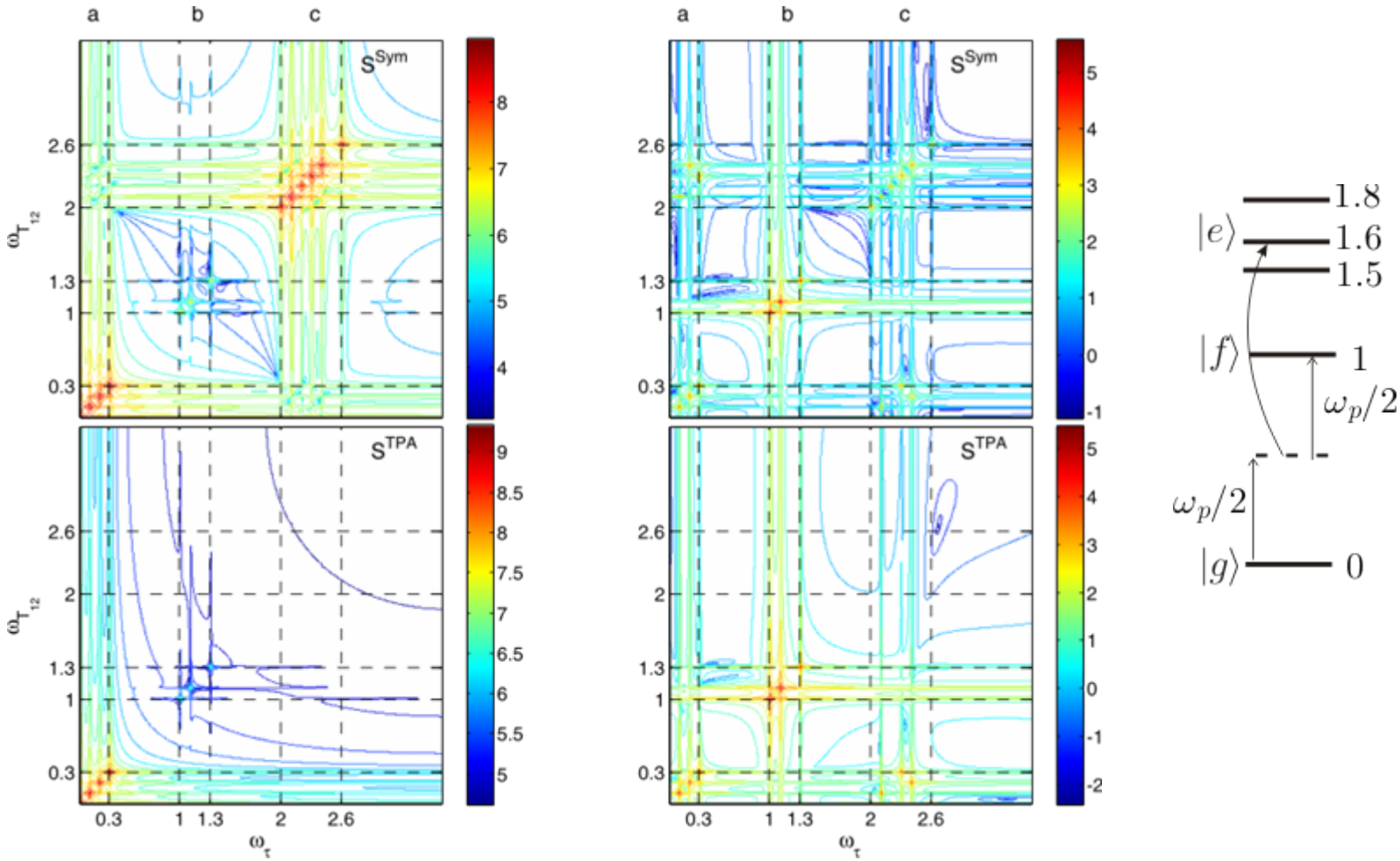

2) For both values of the dephasing rate the TPA and PMP signals miss the (c,c) and (a,a) resonances correspondingly.

TPA with mutually delayed rectangular shaped fields.

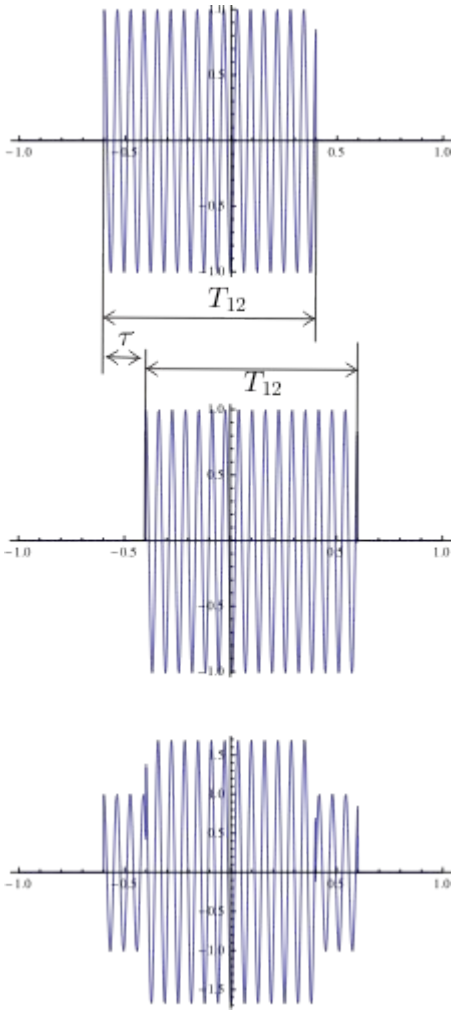

$$E_1(t) = \mathrm{E}_1 \exp(-i\omega_p (t - \tau'/2)/2)\mathrm{rect}\left(\frac{t - \tau'/2 - T_{12}/2}{T_{12}}\right)$$

$$E_2(t) = \mathrm{E}_2 \exp(-i\omega_p (t + \tau'/2)/2)\mathrm{rect}\left(\frac{t + \tau'/2 - T_{12}/2}{T_{12}}\right)$$

$$E_1(t) + E_2(t)$$

TPA with mutually delayed rectangular shaped fields.

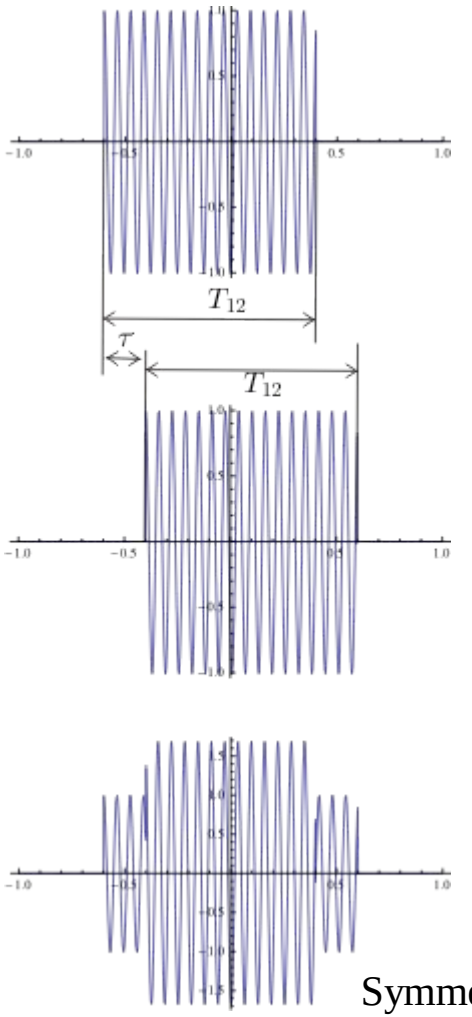

$$E_1(t) = \mathrm{E}_1 \exp(-i\omega_p (t - \tau'/2)/2)\mathrm{rect}\left(\frac{t - \tau'/2 - T_{12}/2}{T_{12}}\right)$$

$$E_2(t) = \mathrm{E}_2 \exp(-i\omega_p (t + \tau'/2)/2)\mathrm{rect}\left(\frac{t + \tau'/2 - T_{12}/2}{T_{12}}\right)$$

Taking into account the following identity:

$$\mathrm{rect}\left(\frac{t_4 - \tau'/2 - T_{12}/2}{T_{12}}\right)\mathrm{rect}\left(\frac{t_2 + \tau'/2 - T_{12}/2}{T_{12}}\right) = \mathrm{rect}\left(\frac{|t_4 - t_2 + \tau'|}{T_{12}}\right)$$

we obtain the field transition amplitudes :

$$\langle E_2(t_4)E_1(t_2)\rangle = \theta(t_4 t_2)E(t_4, t_2, T_{12}) + \theta(t_2 t_4)E(t_2, t_4, T_{12}) =$$

$$= \mathrm{E}_1\mathrm{E}_2 \exp\left(-i\omega_p / 2(t_4 + t_2)\right)\left[\theta(t_4 t_2)\mathrm{rect}\left(\frac{t_4 - t_2}{T_{12} - \tau'}\right) + \theta(t_2 t_4)\mathrm{rect}\left(\frac{t_2 - t_4}{T_{12} + \tau'}\right)\right]$$

$$\langle E_1^{\dagger}(t_3)E_2^{\dagger}(t_1)\rangle = \theta(t_3 t_1)E^{å}(t_3, t_1, T_{12}) + \theta(t_1 t_3)E^{å}(t_1, t_3, T_{12}) =$$

$$= \mathrm{E}_1^{å}\mathrm{E}_2^{å} \exp\left(i\omega_p / 2(t_3 + t_1)\right)\left[\theta(t_3 t_1)\mathrm{rect}\left(\frac{t_3 - t_1}{T_{12} - \tau'}\right) + \theta(t_1 t_3)\mathrm{rect}\left(\frac{t_1 - t_3}{T_{12} + \tau'}\right)\right]$$

Symmetric TPA signal becomes:

$$S_{TPA}^{Sym}(\omega_p / 2, T_{12}, \tau') = -\frac{2\pi^3 N \omega_p^2}{3!\Omega^3}\Im I_{fg}^{å}(\omega_p)\left[-\mathrm{T}_{fg}^{å,2}(\omega_p / 2, T_{12}, \tau') + |\mathrm{T}_{fg}(\omega_p, T_{12}, \tau')|^2\right]$$

τ' independent prefactor

Conclusions

- **We used mutually delayed twin photons to study off-resonant single excited states in a three level model system.**
- **Two detectors measured the change in one of the beams intensity with and without other beam. The symmetric (asymmetric) two-photon absorption was defined as sum (difference) of the detectors readings.**
- **Fully microscopic entangled photon TPA formalism using close time path loop (CTPL) diagrams was developed. Its predictions was compared with proposed before virtual state spectroscopy based on conventional two-photon counting Glauber theory.**
- **For general quantum optical fields CTPL theory yields the signal in terms of Liouville pathways each scaled with corresponding four point optical correlation function. There are two groups of pathways TPA and PMP. The TPA pathways correspond to emission from the double excited states and may be taken into account by the two-photon counting Glauber theory. The PMP pathways are related to emission from the single excited states where the one of the photons creates just an intermediate coherence between the ground and double excited states.**
- **For the degenerate off-resonant case of classical uncorrelated photons the signal PMP = TPA. Asymetric signal vanishes.**

Conclusions

- **For highly correlated entangled photons PMP contribution differs from TPA, as shown in the Fourier spectra.**
- **Dependence of the signal on such adjustable parameters as the delay time and entanglement time makes the single excited states effectively resonant. That is they are off-resonant with respect to the photon frequency but resonant on the spectra defined as the Fourier transform with respect to the delay or entanglement times.**
- **Numerical simulation of the spectra shows that the resonances associated with the single excited state manifold as well as the intra-band transitions within this manifold may be visualized on the correlation spectra. Focusing on different regions in the correlation spectra one can separate PMP and TPA contributions.**
- **Alternatively one can mimic two-photon absorption with entangled photons by using two mutually delayed rectangular shaped optical fields. This shapes up the optical field correlation function so that the two signals differ by delay independent pre-factor giving the same as for twin photons specter (time delay).**